

SEQUENTIAL ACTIVE LEARNING OF LOW-DIMENSIONAL MODEL REPRESENTATIONS FOR RELIABILITY ANALYSIS*

MAX EHRE[†], IASON PAPAIOANNOU[†], BRUNO SUDRET[‡], AND DANIEL STRAUB[†]

Abstract. To date, the analysis of high-dimensional, computationally expensive engineering models remains a difficult challenge in risk and reliability engineering. We use a combination of dimensionality reduction and surrogate modelling termed partial least squares-driven polynomial chaos expansion (PLS-PCE) to render such problems feasible. Standalone surrogate models typically perform poorly for reliability analysis. Therefore, in a previous work, we have used PLS-PCEs to reconstruct the intermediate densities of a sequential importance sampling approach to reliability analysis. Here, we extend this approach with an active learning procedure that allows for improved error control at each importance sampling level. To this end, we formulate an estimate of the combined estimation error for both the subspace identified in the dimension reduction step and surrogate model constructed therein. With this, it is possible to adapt the training set so as to optimally learn the subspace representation and the surrogate model constructed therein. The approach is gradient-free and thus can be directly applied to black box-type models. We demonstrate the performance of this approach with a series of low- (2 dimensions) to high- (869 dimensions) dimensional example problems featuring a number of well-known caveats for reliability methods besides high dimensions and expensive computational models: strongly nonlinear limit-state functions, multiple relevant failure regions and small probabilities of failure.

Key words. Reliability Analysis, Rare event simulation, PLS-PCE, Dimensionality reduction, Active learning, Sequential importance sampling

AMS subject classifications. 62L99, 62P30, 62J02, 65C05

1. Introduction and previous work. An important challenge in the design, analysis and maintenance of engineering systems is the management of the associated uncertainties. It is common practice to analyse engineering systems by employing computational models that aim at representing the physical processes relevant to the system in consideration. These computational models take the form of an input-output mapping. Therein, uncertainty is represented by equipping the model input with an appropriate probabilistic model. Undesirable system responses are defined through a limit-state function (LSF). Reliability analysis is concerned with quantifying the probability of failure, which can be expressed as a d -fold integral of the input probability mass over the failure domain defined by non-positive values of the LSF, where d is the number of uncertain model inputs (see [Section 2](#)). In engineering, target failure probabilities are typically small; hence, reliability analysis requires the estimation of rare event probabilities. Reliability analysis approaches can be categorized into approximation (e.g. the first- and second-order reliability methods FORM and SORM [[66](#), [27](#), [18](#)]) and simulation methods. If the LSF is only weakly nonlinear and the input dimension of the model is moderate, FORM and SORM perform well even for small failure probabilities. The simplest simulation method is the Monte Carlo method [[54](#)]. The Monte Carlo method performs well independent of the problem input dimension, however its performance deteriorates as the failure probability decreases if the computational budget is fixed. Various techniques such as importance sampling (IS) [[13](#), [24](#), [2](#)] and line-sampling [[30](#), [39](#)] have been proposed to mitigate this dependence on the magnitude of the failure probability. More recently, sequential MC methods such as subset simulation [[3](#)] and IS-based sequential methods [[41](#), [42](#), [83](#), [61](#), [68](#), [60](#)] have been used successfully to efficiently solve high-dimensional reliability problems with small failure probabilities. If the computational model is expensive and a hierarchy of increasingly coarse and cheap models is accessible, multilevel and multi-fidelity [[63](#)] MC methods can help alleviate computational cost by performing most model evaluations on the cheaper models (e.g., a discretized differential equation with coarser resolution). In [[79](#)], multilevel MC is combined with subset simulation and recently [[82](#)] have introduced multilevel sequential IS based on the sequential IS approach in [[61](#)]. All of the above-mentioned approaches are designed to work with the probabilistic computational model directly. However, often this model encompasses a numerical solver for (sets of) partial differential equations such that a model evaluation is computationally expensive.

*Submitted to the editors DATE.

Funding: This project was supported by the German Research Foundation (DFG) through Grant STR 1140/6-1 under SPP 1886.

[†]Engineering Risk Analysis Group, Technical University of Munich (max.ehre@tum.de, iason.papaioannou@tum.de, straub@tum.de).

[‡]Chair of Risk, Safety and Uncertainty Quantification, ETH Zürich (sudret@ibk.eth.ch).

48 This has increasingly lead researchers to turn towards surrogate model-based reliability methods. Such
 49 methods attempt to approximate the expensive computational model with a cheap surrogate model, whose
 50 coefficients are identified based on a set of original model evaluations: the training set. [25] uses a polynomial
 51 response surface method for performing reliability analysis as early as 1989. [28] proposes an improved ver-
 52 sion of the response surface method. Since then, a variety of surrogate modelling techniques has been applied
 53 in the context of reliability analysis such as artificial neural networks [57, 34, 71], support vector machines
 54 [33, 12, 11], Gaussian process regression-based models [22, 21] and projection to polynomial bases including
 55 polynomial chaos expansions (PCE) [47, 45, 44, 73] and low-rank tensor approximations [38].

56
 57 *Static, global* surrogate models suffer from a decrease in accuracy in the tails of the model response dis-
 58 tribution such that they are of limited use for reliability analysis. In this context, *static* refers to surrogate
 59 models that are constructed based on a fixed training set and *global* refers to surrogate models that are
 60 trained and evaluated on the entire input space (as opposed to locally con- and re-fined models). Thus, one
 61 can distinguish two strategies to overcome this limitation:

- 62 • *Locality*: Surrogate models are coupled with sequential sampling techniques which serve to focus the
 63 training set and accuracy in the relevant regions around the failure hypersurface [56, 12, 11, 6, 58].
- 64 • *Adaptivity* (in the training set): The training set is augmented with points that are most informative
 65 with respect to the failure probability estimate according to an 'in-fill criterion'. The refined surrogate
 66 model is then used to estimate the probability of failure with a sampling method and a large number
 67 of cheap samples. Such procedures are summarized under the terms active learning (AL) or optimal
 68 experimental design. AL in combination with crude Monte Carlo have been applied in reliability-
 69 based optimization and reliability analysis in [22, 53, 8, 65]. [71] investigates the performance of
 70 splines and neural networks in combination with directional sampling and IS and [21, 14] combine
 71 Gaussian process models with IS. [70] proposes a crude Monte Carlo procedure relying on a Gaussian
 72 process surrogate model with PCE-based mean trend (PCE-Kriging) along with a novel termination
 73 criterion for the AL.

74 Often, both AL and sequential sampling techniques are combined using various combinations of in-fill criteria
 75 and sequential sampling techniques such as adaptive IS [5] and subset simulation [12, 32, 6, 11]. [52] turns
 76 away from surrogate models that naturally provide a measure of prediction uncertainty such as Gaussian
 77 processes or support vector machines and demonstrate how an AL algorithm can be realized with PCE using
 78 a bootstrap estimator of the PCE prediction uncertainty.

79
 80 In spite of a plethora of existing approaches to surrogate-assisted reliability analysis, the literature on high-
 81 dimensional problems ($d \geq 100$) in this context is scarce. [36, 46] propose to perform reliability analysis with
 82 a static, global Kriging model constructed in a low-dimensional linear subspace of the original model input
 83 space, which is identified by the active subspaces method [16] and autoencoders, respectively. Both [36, 46]
 84 apply their methods to moderate-dimensional problems with up to $d = 20$ and $d = 40$ input variables, respec-
 85 tively. [55] uses sliced inverse regression to identify a linear low-dimensional subspace and construct a static,
 86 global PCE in this space based on which they perform reliability analysis directly. [89] develops these ideas
 87 further by combining the active subspace-Kriging model with an AL approach and applies this combination
 88 to a high-dimensional analytical problem of $d = 300$ that possesses a perfectly linear low-dimensional structure.

89
 90 In this work, we propose an importance sampler based on a dimensionality-reducing surrogate model termed
 91 partial least squares-driven PCE (PLS-PCE) [59] to efficiently solve high-dimensional reliability problems with
 92 underlying computationally expensive, nonlinear models and small target probabilities ($\mathcal{O}(10^{-9})$). Similar to
 93 sliced inverse regression and active subspaces, PLS-PCE achieves dimensionality reduction by identifying a
 94 low-dimensional linear subspace of the original input space. Our method is based on [58] but introduces AL
 95 to refine the PLS-PCE approximation in each sequence of the IS procedure. In [58], PLS-PCE models are
 96 reconstructed in each level of a sequential importance sampling (SIS) scheme that is used to gradually shift
 97 the importance density towards the optimal importance density. In this work, we augment this approach
 98 with two novel contributions to rare event simulation of computationally expensive, potentially (but not
 99 necessarily) high-dimensional and nonlinear models:

- 100 1. We demonstrate how to perform active learning with PCE models by deriving an in-fill criterion
 101 from large-sample properties of the PCE coefficient estimates.

102 2. We use projection to linear subspaces to construct efficient surrogate models for high-dimensional
 103 problems and include the subspace estimation error in the in-fill criterion. This means, we are not
 104 only learning the surrogate model but also the subspace itself.

105 Using AL in the context of PLS-PCE-based SIS provides effective error control and benefits from the local
 106 confinement of the learning procedure of each subspace/surrogate model combination to the support of the
 107 current importance density. Constructing local variance estimates for polynomial models in the way we pro-
 108 pose here creates new possibilities to design goal-oriented surrogate modelling approaches that are driven by
 109 adaptive sampling based on such models (where so far, Gaussian processes were the dominant tool).
 110

111 In Section 2, we set up the reliability problem and discuss the crude Monte Carlo sampler of the proba-
 112 bility of failure. Section 3 reviews IS and a variant of SIS [61] that is at the base of our approach. Section 4
 113 introduces PLS-PCE models and their construction. Subsection 5.2 details the theoretical foundations of
 114 active learning of PLS-PCE models within SIS and summarizes our approach. In Section 6, we present com-
 115 prehensive investigations of the method’s performance in two engineering examples and provide a detailed
 116 discussion of the results. Conclusions are given in Section 7.

2. Reliability analysis. Consider a system represented by the computational model $\mathcal{Y} : \mathbb{D}_{\mathbf{X}} \rightarrow \mathbb{R}$ with
 d -dimensional continuous random input vector $\mathbf{X} : \Omega \rightarrow \mathbb{D}_{\mathbf{X}} \subseteq \mathbb{R}^d$, where Ω is the sample space of \mathbf{X} and by
 $F_{\mathbf{X}}(\mathbf{x})$, we denote its joint cumulative distribution function (CDF). \mathcal{Y} maps to the system response $Y = \mathcal{Y}(\mathbf{x})$
 with the model input $\mathbf{x} \in \mathbb{D}_{\mathbf{X}}$. Based on the response Y , unacceptable system states are defined by means
 of the limit-state function (LSF) $\tilde{g}(Y)$. Defining $g(\mathbf{x}) = \tilde{g} \circ \mathcal{Y}(\mathbf{x})$ and introducing the convention

$$g(\mathbf{x}) = \begin{cases} \leq 0, \text{ Failure} \\ > 0, \text{ Safety,} \end{cases}$$

117 the failure event of the system is defined as $F = \{\mathbf{x} \in \mathbb{D}_{\mathbf{X}} : g(\mathbf{x}) \leq 0\}$. The probability of failure is given by
 118 [19]

119 (2.1)
$$p = \mathbb{P}(F) = \int_{\mathbb{D}_{\mathbf{X}}} \mathbb{I}[g(\mathbf{x}) \leq 0] f_{\mathbf{X}}(\mathbf{x}) d\mathbf{x} = \mathbb{E}_{f_{\mathbf{X}}} [\mathbb{I}(g(\mathbf{X}) \leq 0)],$$

120 where $f_{\mathbf{X}}(\mathbf{x}) = \partial^d F / (\partial x_1 \dots \partial x_d)|_{\mathbf{x}}$ is the joint probability density function (PDF) of \mathbf{X} and the indicator
 121 function $\mathbb{I}[\cdot]$ equals 1 if the condition in the argument is true and 0 otherwise. Without loss of generality,
 122 one may formulate an equivalent reliability problem with respect to the standard-normal probability space
 123 using the random vector $\mathbf{U} : \Omega \rightarrow \mathbb{R}^d$. Given an isoprobabilistic transformation $T : \mathbb{D}_{\mathbf{X}} \rightarrow \mathbb{R}^d$, such that
 124 $\mathbf{U} = T(\mathbf{X})$, see, e.g., [29, 48], and defining $G(\mathbf{U}) = g(T^{-1}(\mathbf{U}))$, one can write (2.1) as

125 (2.2)
$$p = \int_{\mathbb{R}^d} \mathbb{I}[G(\mathbf{u}) \leq 0] \varphi_d(\mathbf{u}) d\mathbf{u} = \mathbb{E}_{\varphi_d} [\mathbb{I}(G(\mathbf{U}) \leq 0)],$$

126 where φ_d denotes the d -dimensional independent standard-normal PDF. The crude Monte Carlo estimate of
 127 (2.2) is

128 (2.3)
$$\hat{p}_{\text{MC}} = \frac{1}{n} \sum_{k=1}^n \mathbb{I}[G(\mathbf{u}^k) \leq 0], \quad \mathbf{u}^k \stackrel{i.i.d.}{\sim} \varphi_d,$$

129 where $\mathbf{u}^k \stackrel{i.i.d.}{\sim} \varphi_d$ means that $\{\mathbf{u}^k\}_{k=1}^n$ are n samples that are independent and identically distributed ac-
 130 cording to φ_d . This estimate is unbiased and has coefficient of variation (CoV)

131 (2.4)
$$\delta_{\text{MC}} = \sqrt{\frac{1-p}{np}}.$$

132 The number of samples required to compute \hat{p}_{MC} at a prescribed CoV δ_0 reads

133 (2.5)
$$n_0 = \frac{1-p}{\delta_0^2 p} \stackrel{p \ll 1}{\approx} \frac{1}{\delta_0^2 p}.$$

134 Therefore, crude Monte Carlo is inefficient for estimating rare event probabilities as, by definition, $p \ll 1$ and
 135 thus n_0 becomes large.

136 **3. Sequential importance sampling for rare event estimation.** Variance reduction techniques
 137 can be used to reduce the CoV of the probability estimate at a fixed budget of samples compared to crude
 138 Monte Carlo. One of the most commonly used variance reduction methods is the IS method. Let h be a
 139 density, such that $h(\mathbf{u}) > 0$ whenever $G(\mathbf{u}) \leq 0$. Then, one can rewrite (2.2)

$$140 \quad (3.1) \quad p = \int_{\mathbb{R}^d} \mathbb{I}(G(\mathbf{u}) \leq 0) \overbrace{\frac{\varphi_d(\mathbf{u})}{h(\mathbf{u})}}^{\omega(\mathbf{u})} h(\mathbf{u}) \, d\mathbf{u} = \mathbb{E}_h [\mathbb{I}(G(\mathbf{U}) \leq 0) \omega(\mathbf{U})],$$

141 which leads to the (unbiased) importance sampling estimator

$$142 \quad (3.2) \quad \widehat{p}_{\text{IS}} = \frac{1}{n} \sum_{k=1}^n \mathbb{I}[G(\mathbf{u}^k) \leq 0] \omega(\mathbf{u}^k), \quad \mathbf{u}^k \stackrel{i.i.d.}{\sim} h.$$

143 The efficiency of IS depends intimately on the choice of the IS density h and numerous techniques to construct
 144 it have been put forward. There exists an optimal importance density h^* in the sense that it leads to
 145 $\mathbb{V}[\widehat{p}_{\text{IS}}] = 0$:

$$146 \quad (3.3) \quad h^*(\mathbf{u}) = \frac{1}{p} \mathbb{I}[G(\mathbf{u}) \leq 0] \varphi_d(\mathbf{u}).$$

147 While this result is not immediately useful in estimating p as it requires knowledge of p , it can be used to
 148 guide the selection of a suitable IS function h .

149
 150 The SIS method proposed in [61] selects the IS density sequentially starting from a known distribution
 151 h_0 that is easy to sample from. It relies on a sequence of distributions $\{h_i(\mathbf{u})\}_{i=0}^M$,

$$152 \quad (3.4) \quad h_i(\mathbf{u}) = \frac{\eta_i(\mathbf{u})}{p_i}, \quad i = 1, \dots, M,$$

153 where $\{\eta_i(\mathbf{u})\}_{i=0}^M$ are non-normalized versions of $\{h_i(\mathbf{u})\}_{i=0}^M$ and $\{p_i\}_{i=0}^M$ are the respective normalizing
 154 constants. The goal is to arrive at h_M , which is sufficiently close to h^* based on some criterion, and perform
 155 importance sampling with h_M . To this end, it is necessary to estimate p_M and obtain samples from h_M .
 156 Based on the likelihood ratio of two succeeding non-normalized distributions $\omega_i(\mathbf{u}) = \eta_i(\mathbf{u})/\eta_{i-1}(\mathbf{u})$, we
 157 have

$$158 \quad (3.5) \quad s_i = \frac{p_i}{p_{i-1}} = \int_{\mathbb{R}^d} \frac{\eta_i(\mathbf{u})}{\eta_{i-1}(\mathbf{u})} h_{i-1}(\mathbf{u}) \, d\mathbf{u} = \mathbb{E}_{h_{i-1}} [\omega_i(\mathbf{u})].$$

159 Therefore, an estimate of p_M is given by

$$160 \quad (3.6) \quad \widehat{p}_M = \prod_{i=1}^M \widehat{s}_i \quad \text{with} \quad \widehat{s}_i = \frac{1}{n} \sum_{k=1}^n \omega_i(\mathbf{u}^k), \quad \mathbf{u}^k \stackrel{i.i.d.}{\sim} h_{i-1}.$$

161 Samples from h_i can be obtained using Markov Chain Monte Carlo (MCMC) methods given samples from
 162 h_{i-1} . More precisely, [61] proposes a resample-move scheme in which Markov chain seeds are obtained as
 163 samples from h_{i-1} that are then reweighted (resampled with weights) according to $\omega_i(\mathbf{u})$. In this way, the
 164 seed samples are already approximately distributed according to the stationary distribution of the Markov
 165 chain h_i and long burn-in periods can be avoided. We adopt an adaptive conditional MCMC sampler (aCS)
 166 to perform the move step due to its robust performance in high-dimensional settings. Details can be found
 167 in [61].

168
 169 The h_i are chosen as smooth approximations of h^* using the standard-normal CDF $\Phi(\cdot)$ (compare Fig. 1):

$$170 \quad (3.7) \quad h_i(\mathbf{u}) = \frac{1}{p_i} \Phi\left(-\frac{G(\mathbf{u})}{\sigma_i}\right) \varphi_d(\mathbf{u}) = \frac{1}{p_i} \eta_i(\mathbf{u}),$$

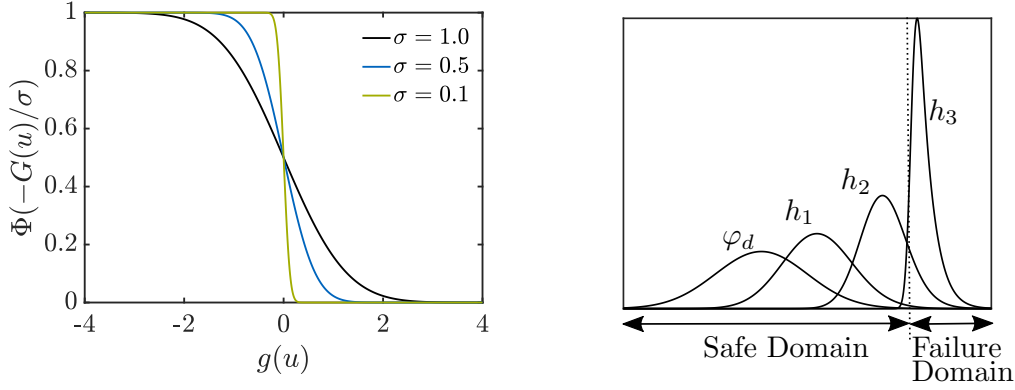


Fig. 1: Smooth approximations to the indicator function $I(g(\mathbf{u}) \leq 0)$ (left) and importance densities $h_i(\mathbf{u}) \propto \Phi(-G(\mathbf{u})/\sigma_i) \varphi_d(\mathbf{u})$ based on this approximation (right).

171 where $p_i = \mathbb{E}_{\varphi_d}[\Phi(-G(\mathbf{U})/\sigma_i)]$ is a normalizing constant and σ_i is the smoothing parameter. Prescribing
 172 $\sigma_0 > \sigma_1 > \dots > \sigma_M$ ensures that the sequence $\{h_i(\mathbf{u})\}_{i=0}^M$ approaches h^* . In each level, to avoid degeneration
 173 of the weights ω_i (meaning ω_i assuming values close to 0 at all current samples), $h_{i-1}(\mathbf{u})$ and $h_i(\mathbf{u})$ cannot
 174 be too different in the sense that they share no support regions on which both have considerable probability
 175 mass. This is avoided by prescribing an upper bound for the estimated coefficient of variation of the weights
 176 $\widehat{\delta}_{w,i} = \widehat{\text{COV}}[\omega_i(\mathbf{U})]$, which provides a criterion for determining σ_i :

$$177 \quad (3.8) \quad \sigma_i = \arg \min_{\sigma \in [0, \sigma_{i-1}]} \left(\widehat{\delta}_{w,i}(\sigma) - \delta_{\text{target}} \right)^2.$$

178 [61] recommends $\delta_{\text{target}} = 1.5$. The algorithm terminates when h_i is close enough to h^* in the sense that

$$179 \quad (3.9) \quad \widehat{\text{COV}} \left[\frac{h^*(\mathbf{U})}{h_i(\mathbf{U})} \right] = \widehat{\text{COV}} \left[\frac{\varphi_d(\mathbf{U}) I(G(\mathbf{U}) \leq 0)}{\varphi_d(\mathbf{U}) \Phi(-G(\mathbf{U})/\sigma_i)} \right] = \widehat{\text{COV}} \left[\frac{I(G(\mathbf{U}) \leq 0)}{\Phi(-G(\mathbf{u})/\sigma_i)} \right] \leq \delta_{\text{target}}.$$

180 The final estimate of $\mathbb{P}(\text{F})$ reads

$$181 \quad (3.10) \quad \widehat{p}_{\text{SIS}} = \widehat{p}_M \widehat{\mathbb{E}}_{\varphi_d} \left[\frac{I(G(\mathbf{U}) \leq 0)}{\eta_M(\mathbf{U})} \right] = \left(\prod_{i=1}^M \widehat{s}_i \right) \frac{1}{n} \sum_{k=1}^n \frac{I(G(\mathbf{u}^k) \leq 0)}{\Phi(-G(\mathbf{u}^k)/\sigma_M)}, \quad \mathbf{u}^k \stackrel{i.i.d.}{\sim} h_M.$$

182 **Algorithm 3.1** summarizes the complete SIS-aCS procedure.

183 4. Partial least squares-based polynomial chaos expansions.

184 **4.1. Polynomial Chaos Expansions.** Polynomial chaos expansions (PCEs) are a tool for forward
 185 modelling the relationship between an input \mathbf{X} and an output $Y = \mathcal{Y}(\mathbf{X})$. With \mathcal{H} , we denote the Hilbert
 186 space of functions that are square-integrable with respect to $f_{\mathbf{X}}$, i.e., $\{v : \mathbb{E}_{f_{\mathbf{X}}}[v(\mathbf{X})^2] < \infty\}$. \mathcal{H} admits an
 187 inner product of two functions $v, w \in \mathcal{H}$:

$$188 \quad (4.1) \quad \langle v, w \rangle_{\mathcal{H}} = \mathbb{E}_{f_{\mathbf{X}}(\mathbf{x})}[v(\mathbf{X})w(\mathbf{X})] = \int_{\mathbb{R}^d} v(\mathbf{x})w(\mathbf{x})f_{\mathbf{X}}(\mathbf{x})d\mathbf{x}.$$

189 Let $\{v_j(\mathbf{X}), j \in \mathbb{N}\}$ be a complete and orthonormal basis of \mathcal{H} so that $\langle v_j, v_\ell \rangle_{\mathcal{H}} = \delta_{j\ell}$ and let $\mathcal{Y} \in \mathcal{H}$. Then,

$$190 \quad (4.2) \quad \mathcal{Y}(\mathbf{X}) = \sum_{j=0}^{\infty} b_j v_j(\mathbf{X}),$$

191 where the coefficients b_j are defined by projecting \mathcal{Y} on the basis:

$$192 \quad (4.3) \quad b_j = \langle \mathcal{Y}, v_j \rangle_{\mathcal{H}}, \quad j \in \mathbb{N}.$$

Algorithm 3.1 SIS-aCS [61]

```

1: Input LSF  $G(\mathbf{u})$ , target CoV  $\delta_{\text{target}}$ , samples per level  $n$ , input dimension  $d$ , burn-in period  $b$ , max.
   iterations  $i_{\text{max}}$ 
2:
3: Set  $i = 0$ ,  $\sigma_0 = \infty$ ,  $h_0(\mathbf{u}) = \varphi_d(\mathbf{u})$ 
4: Sample  $\mathbf{U}_0 = \{\mathbf{u}^k, k = 1, \dots, n\} \in \mathbb{R}^{n \times d}$  ▷  $\mathbf{u}^k \stackrel{i.i.d.}{\sim} h_0(\mathbf{u})$ 
5: Compute  $\mathbf{G}_0 = G(\mathbf{U}_0) \in \mathbb{R}^{n \times 1}$ 
6: for  $i \leftarrow 1, i_{\text{max}}$  do
7:    $i \leftarrow i + 1$ 
8:   Compute  $\sigma_i$  according to (3.8)
9:   Compute weights  $\boldsymbol{\omega}_i = \{\Phi[-\mathbf{G}_{i-1}/\sigma_i]/\Phi[-\mathbf{G}_{i-1}/\sigma_{i-1}], k = 1, \dots, n\} \in \mathbb{R}^{n \times 1}$ 
10:  Compute  $\hat{s}_i$  according to (3.6).
11:   $\mathbf{U}_{i-1} \leftarrow$  draw weighted resample from  $\mathbf{U}_{i-1}$  with weights  $\boldsymbol{\omega}_i$  ▷ sample with replacement
12:   $(\mathbf{U}_i, \mathbf{G}_i) =$  MCMC-aCS( $\mathbf{U}_{i-1}, \mathbf{G}_{i-1}, b$ ) ▷ Details on MCMC-aCS in [61]
13:  if (3.9) then
14:    break
15: Set  $M \leftarrow i$ 
16: Estimate failure probability  $\hat{p}_{\text{SIS}} = \left(\prod_{i=1}^M \hat{s}_i\right) \frac{1}{n} \sum_{k=1}^n \frac{\mathbb{I}(\mathbf{G}_M^k \leq 0)}{\Phi(-\mathbf{G}_M^k/\sigma_M)}$  ▷ (3.10)
17: return  $\mathbf{U}_M, \mathbf{G}_M, \hat{p}_{\text{SIS}}$ .
```

193 Since $\mathcal{Y} \in \mathcal{H}$, the truncation

$$194 \quad (4.4) \quad \hat{\mathcal{Y}}_n(\mathbf{X}) = \sum_{j=0}^n b_j v_j(\mathbf{X})$$

195 asymptotically converges to \mathcal{Y} as $n \rightarrow \infty$ in the mean square sense. [87] demonstrates how to construct
 196 complete orthonormal bases of \mathcal{H} as polynomial families for various standard input distribution types. In
 197 particular, if $F_{\mathbf{X}}(\mathbf{x}) = \Phi_d(\mathbf{x})$, where Φ_d denotes the d -variate independent standard-normal CDF, the ten-
 198 sorized, normalized probabilist's Hermite polynomials

$$199 \quad (4.5) \quad \Psi_{\mathbf{k}}(\mathbf{U}) = \prod_{i=1}^d \psi_{k_i}(U_i)$$

200 form a complete orthonormal basis of \mathcal{H} . $\{\psi_j(U), j \in \mathbb{N}\}$ are the univariate, normalized (probabilist's)
 201 Hermite polynomials and $\mathbf{k} = (k_1, \dots, k_d) \in \mathbb{N}^d$. By means of the isoprobabilistic transformation $T : \mathbf{X} \rightarrow \mathbf{U}$
 202 introduced in the previous section, we define PCEs in standard-normal space for the remainder of the paper.
 203 The PCE of maximum total order p reads

$$204 \quad (4.6) \quad \hat{\mathcal{Y}}_p(\mathbf{U}) = \sum_{|\mathbf{k}| \leq p} b_{\mathbf{k}} \Psi_{\mathbf{k}}(\mathbf{U}).$$

205 The total number of basis functions in the PCE, P , depends on the input dimension d and the maximum
 206 total polynomial order p :

$$207 \quad (4.7) \quad P = \binom{d+p}{p}.$$

208 The projection in (4.3) can be transformed into an equivalent ordinary least squares (OLS) problem [7].
 209 PCEs become computationally intractable if d is large, i.e., they cannot be used for problems with high-
 210 dimensional input due to the sheer number of basis functions and corresponding coefficients. In particular,
 211 the computation is rendered infeasible by the necessary number of operations to compute the set of P multi-
 212 indices and the necessary number of model evaluations to obtain meaningful estimates of the coefficients.
 213 Solution strategies to overcome these limitations (at least partially) include a hyperbolic truncation of the

214 index set (this means to replace the condition on the ℓ_1 -norm in (4.6), $|\mathbf{k}| \leq p$, with one on a general ℓ_q -norm
 215 of $|\mathbf{k}|_\alpha = (\sum_{i=1}^d p_i^q)^{1/q} \leq p$ with $q < 1$) or enforcing a maximum interaction order (i.e., a maximum number
 216 of non-zero entries in \mathbf{k}) [9]. These approaches result in more parsimonious models and allow for PCEs
 217 to be applied in higher-dimensional problems, however do so at the cost of decreased model expressivity.
 218 Sparsity-inducing solvers have been proposed to relax the dimensionality constraint imposed by the size of
 219 the regression problem. Approaches may be based on a variety of solvers for the ℓ_1 -regularized least squares
 220 problem such as least-angle regression (LARS) that is used for PCEs in [10], compressive sensing [88] and
 221 orthogonal matching pursuit [62, 76, 20] as well as sparse Bayesian learning methods [75, 35, 69, 78]. For a
 222 comprehensive overview, the reader is referred to the recent literature review and benchmark study [51, 50].

223 **4.2. Basis adaptation via partial least squares.** In order to obtain a parsimonious yet expressive
 224 model, we turn to low-dimensional model representations rather than sparse solutions to the full-dimensional
 225 model. To achieve this, the PCE representation is rotated onto a new basis defined by the variables $\mathbf{Z} = \mathbf{Q}^T \mathbf{U}$,
 226 where $\mathbf{Q} \in \mathbb{R}^{d \times d}$ and $\mathbf{Q}^T \mathbf{Q} = \mathbf{I}$, with \mathbf{I} denoting the identity matrix. This has first been proposed in [74].
 227 The PCE with respect to the novel basis reads

$$228 \quad (4.8) \quad \hat{\mathcal{Y}}_p^{\mathbf{Q}}(\mathbf{U}) = \sum_{|\mathbf{k}| \leq p} a_{\mathbf{k}} \Psi_{\mathbf{k}}(\mathbf{Z}) = \sum_{|\mathbf{k}| \leq p} a_{\mathbf{k}} \Psi_{\mathbf{k}}(\mathbf{Q}^T \mathbf{U}).$$

229 With \mathbf{U} a standard-normal random vector and \mathbf{Q} an orthogonal matrix, \mathbf{Z} is a standard-normal random
 230 vector. Therefore, both original and transformed input space possess the same PCE basis, namely the
 231 probabilist's Hermite polynomials. Merely, a new set of coefficients $a_{\mathbf{k}}$ enters the formulation in the adapted
 232 basis. The columns of \mathbf{Q} define linear combinations of the original input. We seek to choose \mathbf{Q} such that
 233 most of the relevant information to construct an accurate surrogate \mathcal{Y} is captured in the first m directions,
 234 where $m < d$ leads to dimensionality reduction. We retain only these first m columns of \mathbf{Q} in the matrix \mathbf{Q}_m
 235 and define a corresponding PCE of reduced dimension as

$$236 \quad (4.9) \quad \hat{\mathcal{Y}}_p^{\mathbf{Q}_m}(\mathbf{U}) = \sum_{|\mathbf{k}| \leq p} a_{\mathbf{k}} \Psi_{\mathbf{k}}(\mathbf{Q}_m^T \mathbf{U}),$$

237 where $\mathbf{k} \in \mathbb{N}^m$. [74] computes the basis adaptation \mathbf{Q}_m by evaluating first- or second-order PCE coeffi-
 238 cients only with a sparse-grid numerical quadrature. [77] couples this approach with compressive sensing to
 239 simultaneously identify \mathbf{Q}_m and the PCE coefficients in the subspace. In [59], we show that important direc-
 240 tions can be identified efficiently based on a set of original function evaluations via partial least squares (PLS).
 241

242 PLS establishes a linear relationship between variables \mathbf{U} and Y based on $n_{\mathcal{E}}$ observations of both quantities
 243 [85]. By $\mathbf{U}_{\mathcal{E}} \in \mathbb{R}^{n_{\mathcal{E}} \times d}$, we denote the matrix of $n_{\mathcal{E}}$ observations of \mathbf{U} and by $\mathbf{Y}_{\mathcal{E}} \in \mathbb{R}^{n_{\mathcal{E}} \times 1}$ we denote the
 244 corresponding vector of scalar responses. PLS sequentially identifies m latent components $\{\mathbf{t}_j\}_{j=1}^m$, where
 245 $\mathbf{t}_j \in \mathbb{R}^{n_{\mathcal{E}} \times 1}$ such that they have maximum covariance with $\mathbf{Y}_{\mathcal{E}}$. After determining each \mathbf{t}_j , PLS assumes
 246 a linear relationship between \mathbf{t}_j and $\mathbf{Y}_{\mathcal{E}}$ and evaluates the corresponding coefficient a_j of \mathbf{t}_j by OLS. After
 247 each iteration, the matrices $\mathbf{U}_{\mathcal{E}}$ and $\mathbf{Y}_{\mathcal{E}}$ are deflated by the contribution of the j -th PLS-component. Com-
 248 ponents are extracted until a certain error criterion is met, which can be formulated, e.g., through the norm
 249 of the residual response vector or via cross-validation. Dimensionality-reducing regression methods such als
 250 PLS-based regression are known to shrink the regression coefficients towards zero to produce biased estimates
 251 in exchange for reducing the estimator variances (bias-variance-tradeoff). In this way, these dimensionality-
 252 reducing methods are able to produce smaller overall mean squared estimation errors. (see, e.g., [17] for PLS).
 253

254 The nonlinear version of PLS in turn relaxes the assumption of a linear relationship between latent compo-
 255 nent and the response. A number of nonlinear PLS algorithms have been proposed [67]. Here we employ the
 256 approach of Refs. [84, 4] that introduces an additional loop into the algorithm for running a Newton-Raphson
 257 procedure iterating between the current latent component and the response. Ultimately, we are interested
 258 in computing the orthogonal transformation matrix \mathbf{Q}_m in (4.9). PLS produces two different matrices \mathbf{R}
 259 and \mathbf{W} that are suitable to this end, which motivates two different flavors of PLS-PCE. In PLS-PCE-R as
 260 proposed in [59] (see Subsection 4.3), each nonlinear relationship between the $\{\mathbf{t}_j\}_{j=1}^m$ and the response is
 261 modelled as a univariate PCE. The coefficients of these univariate PCEs are computed simultaneously with
 262 the latent structure and the resulting model is a sum of univariate PCEs. Alternatively, the univariate PCEs

263 are discarded after the PLS-PCE algorithm terminates and a multivariate (sparse) PCE is constructed in the
 264 subspace formed by the so-called weights $\{\mathbf{w}_j\}_{j=1}^m$ leading to PLS-PCE-W (see [Subsection 4.4](#)).

265 **4.3. PLS-PCE-R.** PLS-PCE-R identifies m latent components and for each component, it returns
 266 the direction \mathbf{r}_j and the univariate PCE along this direction. The univariate PCEs are defined by their
 267 polynomial orders $\{q_j\}_{j=1}^m$ and the associated coefficient vectors $\{\mathbf{a}_j\}_{j=1}^m$. The polynomial order is identified
 268 with leave-one-out cross validation [15]. For each (j -th) latent component, the nonlinear PLS iteration is
 269 repeated for different polynomial orders and q_j is chosen as the order minimizing the leave-one-out error.
 270 The PLS-PCE-R model reads

$$271 \quad (4.10) \quad \hat{\mathcal{Y}}(\mathbf{u}) = \hat{a}_0 + \sum_{j=1}^m (\hat{\mathbf{a}}_j^{q_j})^\top \psi_{q_j} [\mathbf{r}_j^\top (\mathbf{u} - \boldsymbol{\mu}_{\mathbf{U}})],$$

272 where $\hat{a}_0 = \hat{\mathbb{E}}[\mathbf{Y}]$, $\psi_{q_j}(\mathbf{U})$ is a vector function assembling the evaluations of the one-dimensional Hermite
 273 polynomials up to order q_j and $\boldsymbol{\mu}_{\mathbf{U}}$ is the columnwise sample mean of $\mathbf{U}_{\mathcal{E}}$. The model structure is illustrated
 274 in [Fig. 2](#). The PLS directions \mathbf{r}_j can be evaluated in terms of the PLS weights \mathbf{w}_j and loads \mathbf{p}_j through the
 275 following recursive relation [31]

$$276 \quad (4.11) \quad \begin{aligned} \mathbf{r}_1 &= \mathbf{w}_1 \\ \mathbf{r}_j &= \mathbf{w}_j - \mathbf{r}_{j-1} (\mathbf{p}_{j-1}^\top \mathbf{w}_j). \end{aligned}$$

277 $\mathbf{R} = [\mathbf{r}_1, \dots, \mathbf{r}_m] \in \mathbb{R}^{d \times m}$ is a matrix collecting all PLS directions. \mathbf{R} is not necessarily orthogonal, i.e., in
 278 general $\mathbf{R}^\top \mathbf{R} \neq \mathbf{I}$. However, in [59] it is shown that $\mathbf{R}^\top \mathbf{R} \approx \mathbf{I}$ when $n_{\mathcal{E}}$ is large and $\mathbf{U}_{\mathcal{E}}^\top \mathbf{U}_{\mathcal{E}}$ is diagonal, which
 279 is the case if $\mathbf{U}_{\mathcal{E}}$ is drawn from φ_d . In this case, (4.10) is equivalent to a PCE of the form (4.9), where only
 280 main effects in the latent components are considered.

281 **4.4. PLS-PCE-W.** PLS-PCE-W defines \mathbf{W} as basis of the subspace rather than \mathbf{R} , where $\mathbf{W} =$
 282 $[\mathbf{w}_1, \dots, \mathbf{w}_m] \in \mathbb{R}^{d \times m}$. Within linear PLS, the columns of \mathbf{W} form an orthogonal basis. Within nonlinear
 283 PLS, the Newton-Raphson step may introduce deviations from orthogonality, which are however negligible in
 284 all tested examples. The univariate PCEs obtained through the Newton-Raphson step will be optimal with
 285 respect to \mathbf{R} , not \mathbf{W} . Thus, in PLS-PCE-W these univariate polynomials are discarded once \mathbf{W} is identified
 286 and a multivariate (sparse) PCE is constructed in the subspace defined by \mathbf{W} using least-angle regression and
 287 a hyperbolic truncation scheme for the multivariate PCE basis as proposed by [10]. In this way PLS-PCE-
 288 W achieves more flexibility compared to PLS-PCE-R by including interactions of the latent components in
 289 exchange for a departure from optimality in the match between latent component and surrogate model. In
 290 analogy to (4.9), the PLS-PCE-W model reads

$$291 \quad (4.12) \quad \hat{\mathcal{Y}}(\mathbf{u}) = \hat{a}_0 + \sum_{\mathbf{k} \in \boldsymbol{\alpha}} \hat{a}_{\mathbf{k}} \Psi_{\mathbf{k}} [\mathbf{W}^\top (\mathbf{u} - \boldsymbol{\mu}_{\mathbf{U}})],$$

292 where $\boldsymbol{\alpha} \in \mathbb{N}^{P \times d}$ is the multi-index set, which indicates the polynomial orders of the d univariate polynomials
 293 in each of the P multivariate polynomials as obtained with LARS. Both PLS-PCE-R and PLS-PCE-W are
 294 summarized in [Algorithm 4.1](#). In the following, we will use the PLS-PCE-W model as we observed a superior
 295 performance for this model compared to PLS-PCE-R models in the context of the proposed approach.

296 **5. Learning PLS-PCE models in each SIS level.**

297 **5.1. The sequential subspace importance sampler.** We recently proposed to reconstruct low-
 298 dimensional PLS-PCE-W models in each level of SIS to improve the tractability of high-dimensional reli-
 299 ability analysis with computationally expensive models [58]. We term this approach sequential subspace
 300 importance sampling or SSIS. The efficiency of SIS benefits from surrogate modelling through a considerable
 301 reduction of required model evaluations. The PLS-PCE model alone, being a global surrogate model, is a
 302 relatively limited tool for reliability analysis. Combining it with SIS provides the means to sequentially move
 303 the training set towards relevant regions in the input space and thereby renders difficult reliability problems
 304 accessible to surrogate modelling. At the i -th SSIS level, a new *local* training set is sampled from the current
 305 importance density h_i through a resampling step on the N available samples from h_i . The new *local* training
 306 set is appended to the *global* training set comprising earlier designs from levels 1 through $i - 1$. Based on the

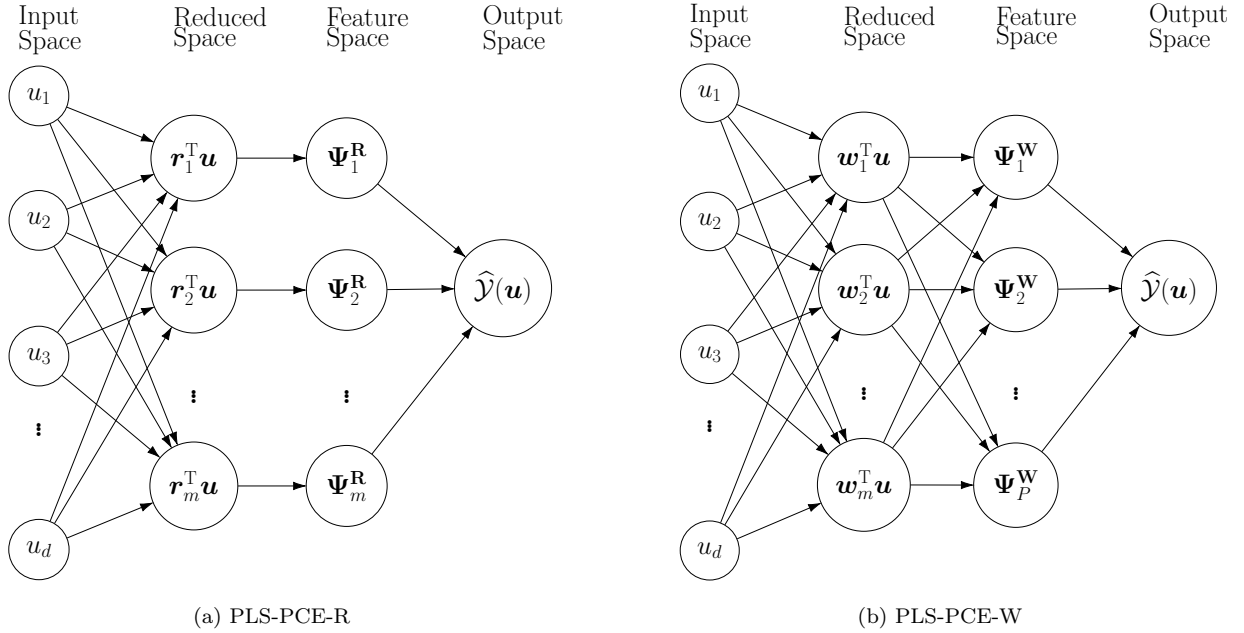


Fig. 2: Structure of two different PLS-PCE models, where $\Psi_j^W = \Psi_{\alpha_j}$ as defined in (4.12) and $\Psi_j^R = (\hat{\mathbf{a}}_j^{q_j})^T \psi_{q_j}$ as seen from (4.10). Essential differences exist in the choice of the reduced space basis (layer 2) and the modelling of cross-terms when mapping from reduced to feature space (layers 2 & 3) with PLS-PCE-W (b).

307 updated *global* training set, a new PLS-PCE model is constructed and SIS is rerun for $i + 1$ levels from h_0 to
 308 obtain samples for the next *local* training set. Due to this restart, it is sensible to let previously used local
 309 training sets remain in the global training set such that the i -th surrogate model accurately predicts the LSF
 310 output along the entire path of samples moving from the nominal distribution h_0 to h_i . The restart itself
 311 incurs no additional LSF evaluations and serves to stabilize the method: Without restart, the computation
 312 of σ_{i+1} according to (3.8) is based on two different surrogate models: the most recent model constructed
 313 in level i appears in the numerator of the sample CoV of the weights and the model constructed in level
 314 $i - 1$ appears in the denominator. These models may however be too different from one another to admit a
 315 solution in (3.8), i.e., to achieve the prescribed CoV δ_{target} between two subsequent IS densities.

316

317 In an additional step, before propagating the intermediate importance density to the next level of the SSIS
 318 algorithm, we introduce AL. This ensures a prescribed surrogate model accuracy in regions of high probability
 319 mass of the current sampling density. In turn, this refined surrogate model is used to propagate samples to
 320 the next level. When the underlying SIS algorithm reaches convergence, a final AL procedure, performed over
 321 samples of the final importance density, ensures that the probability of failure is estimated with a surrogate
 322 model that captures the failure hypersurface well. This approach is termed adaptive sequential subspace
 323 importance sampling or ASSIS.

324

325 Active learning has emerged in the late 1980s as a subfield of machine learning [72] and was known in
 326 the statistical theory of regression as optimal experimental design since the early 1970s [26]. At its heart is
 327 the idea that supervised learning algorithms can perform better if allowed to choose their training data. We
 328 consider a ‘pool-based sampling’ variant of active learning, in which a large pool of unlabeled data points
 329 are made available to the algorithm. Within SIS, one has n samples from h_i available in the i -th level. The
 330 algorithm then selects n_{add} points that are labeled (i.e. for which the LSF is evaluated) and added to the
 331 training set based on a measure of information gain. This measure typically takes the form of a learning

Algorithm 4.1 PCE-driven PLS algorithm [59]

```

1: Input Input matrix  $\mathbf{U}_\mathcal{E}$  and output vector  $\mathbf{Y}_\mathcal{E}$ , maximum polynomial order  $p$ 
2:
3: Set  $\mathbf{E} = \mathbf{U}_\mathcal{E} - \boldsymbol{\mu}_\mathbf{U}$ ,  $\mathbf{F} = \mathbf{Y}_\mathcal{E} - \boldsymbol{\mu}_\mathbf{Y}$ ,  $\epsilon_w = 10^{-3}$ ,  $\epsilon_y = 10^{-3}$ ,  $j = 1$ 
4: repeat
5:   Compute weight  $\mathbf{w}_j^0 = \mathbf{E}^\top \mathbf{F} / \|\mathbf{E}^\top \mathbf{F}\|$ 
6:   for  $q \leftarrow 1, p$  do
7:     Set  $\mathbf{w}_j^q = \mathbf{w}_j^0$ 
8:     repeat
9:       Compute score  $\mathbf{t}_j^q = \mathbf{E} \mathbf{w}_j^q$ 
10:      Fit a 1D PCE of order  $q$   $\hat{\mathbf{a}}_j^q \leftarrow \text{fit} [\mathbf{F} = (\mathbf{a}_j^q)^\top \boldsymbol{\psi}_q(\mathbf{t}_j^q) + \boldsymbol{\epsilon}]$ 
11:      Set  $\hat{\mathcal{M}}_j^q(t) = (\hat{\mathbf{a}}_j^q)^\top \boldsymbol{\psi}_q(\mathbf{t}_j^q)(t)$ 
12:      Compute the error  $\mathbf{e} = \mathbf{F} - (\hat{\mathbf{a}}_j^q)^\top \boldsymbol{\psi}_q(\mathbf{t}_j^q)$ 
13:      Compute  $\Delta \mathbf{w}_j^q = (\mathbf{A}^\top \mathbf{A})^{-1} \mathbf{A}^\top \mathbf{e}$  with  $\mathbf{A} = \nabla_{\mathbf{w}} (\hat{\mathbf{a}}_j^q)^\top \boldsymbol{\psi}_q(\mathbf{E} \mathbf{w})$ 
14:      Set  $\mathbf{w}_j^q \leftarrow \mathbf{w}_j^q + \Delta \mathbf{w}_j^q$ 
15:      Normalize  $\mathbf{w}_j^q \leftarrow \mathbf{w}_j^q / \|\mathbf{w}_j^q\|$ 
16:     until  $\|\Delta \mathbf{w}_j^q\|$  is smaller than  $\epsilon_w$ 
17:     Evaluate the relative leave-one-out error  $\epsilon_{LOO}^q$  as in [10]
18:   Set  $\{q_j, \hat{\mathbf{a}}_j^{q_j}, \mathbf{w}_j^{q_j}\}$  as the triple  $\{q, \hat{\mathbf{a}}_j^q, \mathbf{w}_j^q\}$  with the smallest  $\epsilon_{LOO}^q$ 
19:   Compute score:  $\mathbf{t}_j^{q_j} = \mathbf{E} \mathbf{w}_j^{q_j}$ 
20:   Compute load:  $\mathbf{p}_j^{q_j} = \mathbf{E}^\top \mathbf{t}_j^{q_j} / ((\mathbf{t}_j^{q_j})^\top \mathbf{t}_j^{q_j})$ 
21:   Deflate:  $\mathbf{E} \leftarrow \mathbf{E} - \mathbf{t}_j^{q_j} (\mathbf{p}_j^{q_j})^\top$ ,  $\mathbf{F} \leftarrow \mathbf{F} - (\hat{\mathbf{a}}_j^{q_j})^\top \boldsymbol{\psi}_{q_j}(\mathbf{t}_j^{q_j})$ 
22:    $j \leftarrow j + 1$ 
23: until change in  $\|\mathbf{F}\|$  is smaller than  $\epsilon_y$ 
24: Compute  $\mathbf{R} = [\mathbf{r}_1, \mathbf{r}_2, \dots, \mathbf{r}_m]$  according to (4.11) ▷ For the  $R$ -based version of PLS-PCE
25: Build  $\hat{\mathcal{Y}}(\mathbf{u})$  according to (4.10)
26: Gather  $\mathbf{W} = [\mathbf{w}_1, \mathbf{w}_2, \dots, \mathbf{w}_m]$  ▷ For the  $W$ -based version of PLS-PCE
27: Build  $\hat{\mathcal{Y}}(\mathbf{u})$  according to (4.12) and [10]
28: return  $\mathbf{R}/\mathbf{W}$ ,  $\hat{\mathcal{Y}}(\mathbf{u})$ 

```

332 function \mathcal{L} that is maximized over the sample pool to perform selection. The learning function employed in
333 the context of SSIS is discussed in Subsection 5.2.

334

335 The probability of failure estimator for SSIS/ASSIS is analogous to (3.10) with the difference that SIS
336 is performed with an LSF approximation \hat{G} that is based on the final surrogate model:

$$337 \quad (5.1) \quad \hat{p} = \left(\prod_{i=1}^M \hat{s}_i \right) \frac{1}{n} \sum_{k=1}^n \frac{\mathbb{I}(\hat{G}(\mathbf{u}^k) \leq 0) \varphi_d(\mathbf{u}^k)}{\eta_M(\mathbf{u}^k)}, \quad \mathbf{u}^k \stackrel{i.i.d.}{\sim} h_M.$$

338 The ratio of normalizing constants $\{\hat{s}_i\}_{i=1}^M$ are estimated as

$$339 \quad (5.2) \quad \hat{s}_i = \frac{1}{n} \sum_{k=1}^n \hat{\omega}_i(\mathbf{u}^k) = \frac{1}{n} \sum_{k=1}^n \frac{\Phi(-\hat{G}(\mathbf{u}^k)/\sigma_i)}{\Phi(-\hat{G}(\mathbf{u}^k)/\sigma_{i-1})}, \quad \mathbf{u}^k \stackrel{i.i.d.}{\sim} h_i.$$

340 The SSIS/ASSIS algorithms are stopped based on a similar criterion as for SIS given in (3.9):

$$341 \quad (5.3) \quad \widehat{\text{COV}} \left[\frac{\mathbb{I}(\hat{G}(\mathbf{U}) \leq 0)}{\Phi(-\hat{G}(\mathbf{U})/\sigma_i)} \right] \leq \delta_{\text{target}}.$$

342 Fig. 3 depicts flow diagrams of the SSIS and ASSIS algorithms.

343 **5.2. Active learning of low-dimensional model representations.** In the context of SSIS, the
 344 learning function \mathcal{L} should express the prediction uncertainty at each sample of the current IS density for a
 345 given PLS-PCE-W surrogate. This prediction uncertainty is due to the estimation of both the subspace and
 346 the surrogate model with a finite-sized training set. We describe this uncertainty with the variance of the
 347 LSF based on the surrogate model conditional on \mathbf{u} , $\mathbb{V}[\widehat{G}|\mathbf{U} = \mathbf{u}]$. Note that, whenever the distribution with
 348 respect to which $\mathbb{E}[\cdot]$ or $\mathbb{V}[\cdot]$ are evaluated is not made explicit as a subscript, it is implicitly assumed as the
 349 distribution of the argument. For example, $\mathbb{V}[\widehat{G}|\mathbf{U} = \mathbf{u}] = \mathbb{V}_{f_{\widehat{G}|\mathbf{u}}}[\widehat{G}|\mathbf{U} = \mathbf{u}]$.

350
 351 Let $\boldsymbol{\xi}_0 = \mathbf{a} \in \mathbb{R}^{P \times 1}$ and $\boldsymbol{\xi}_j = \mathbf{w}_j \in \mathbb{R}^{d \times 1}$, $j = 1, \dots, m$, such that $\boldsymbol{\xi} = [\boldsymbol{\xi}_0^\top, \boldsymbol{\xi}_1^\top, \dots, \boldsymbol{\xi}_m^\top]^\top \in \mathbb{R}^{(md+P) \times 1}$
 352 is the collection of all $md + P$ model parameters. Further, let $\boldsymbol{\xi}^*$ denote their corresponding point estimates
 353 returned by [Algorithm 4.1](#). The first-order expansion of $\widehat{\mathbb{V}}[\widehat{G}|\mathbf{u}]$ around $\boldsymbol{\xi}^*$ reads

$$354 \quad (5.4) \quad \widehat{\sigma}_{\widehat{G}}^2(\mathbf{u}) = \widehat{\mathbb{V}}[\widehat{G}|\mathbf{u}] \approx \left[\frac{\partial \widehat{G}}{\partial \boldsymbol{\xi}} \right]_{\boldsymbol{\xi}=\boldsymbol{\xi}^*}^\top \widehat{\boldsymbol{\Sigma}}_{\boldsymbol{\xi}\boldsymbol{\xi}} \left[\frac{\partial \widehat{G}}{\partial \boldsymbol{\xi}} \right]_{\boldsymbol{\xi}=\boldsymbol{\xi}^*},$$

355 where $\widehat{\boldsymbol{\Sigma}}_{\boldsymbol{\xi}\boldsymbol{\xi}}$ is an estimate of the parameter covariance matrix. Next, we neglect the pairwise cross-covariance
 356 of PCE coefficients \mathbf{a} and the subspace components \mathbf{w}_j and consider

$$357 \quad (5.5) \quad \widehat{\sigma}_{\widehat{G}}^2(\mathbf{u}) = \widehat{\mathbb{V}}[\widehat{G}|\mathbf{u}] \approx \sum_{j=0}^m \left[\frac{\partial \widehat{G}(\mathbf{u}, \boldsymbol{\xi})}{\partial \boldsymbol{\xi}_j} \right]_{\boldsymbol{\xi}_j=\boldsymbol{\xi}_j^*}^\top \widehat{\boldsymbol{\Sigma}}_{\boldsymbol{\xi}_j \boldsymbol{\xi}_j} \left[\frac{\partial \widehat{G}(\mathbf{u}, \boldsymbol{\xi})}{\partial \boldsymbol{\xi}_j} \right]_{\boldsymbol{\xi}_j=\boldsymbol{\xi}_j^*}$$

358 This significantly reduces the number of $\boldsymbol{\Sigma}_{\boldsymbol{\xi}\boldsymbol{\xi}}$ -entries that have to be estimated, namely from $P^2 + 2Pmd + m^2 d^2$
 359 to $P^2 + md^2$. More importantly, the coefficients of the PCE, $\boldsymbol{\xi}_0$, are obtained with linear regression while
 360 the subspace, $\{\boldsymbol{\xi}_j\}_{j=1}^m$, is obtained in the inner loop of [Algorithm 4.1](#) with nonlinear regression. Due to this
 361 sequential estimation of the $\{\boldsymbol{\xi}_j\}_{j=0}^m$, there is no straightforward way of obtaining an estimate of the full
 362 covariance matrix. In particular, we are not aware of such an estimate for the parameters of nonlinear PLS.
 363 Hence, this simplification is not only convenient but also necessary in practice. We do observe, however,
 364 that the off-diagonal elements of the estimated component-wise cross-covariance matrices $\widehat{\boldsymbol{\Sigma}}_{\boldsymbol{\xi}_j \boldsymbol{\xi}_j}$ are several
 365 orders of magnitude smaller compared to the the main diagonal elements. This indicates that the model
 366 uncertainty estimate is dominated by parameter variances. In fact, in a more radical approach that remains
 367 unexplored in this work, one may consider parameter variances only (i.e., only $P + md$ entries of the full
 368 covariance matrix are retained). Such an approach is, e.g., used in [\[64\]](#). Under some regularity conditions,
 369 the estimator $\boldsymbol{\xi}_j^*$ is consistent [\[86\]](#) and converges in distribution to a multivariate Gaussian distribution with
 370 mean $\boldsymbol{\xi}_j$ and covariance $\boldsymbol{\Sigma}_{\boldsymbol{\xi}_j \boldsymbol{\xi}_j}$. In analogy with linear regression, an estimate of $\boldsymbol{\Sigma}_{\boldsymbol{\xi}_j \boldsymbol{\xi}_j}$ is given through

$$371 \quad (5.6) \quad \widehat{\boldsymbol{\Sigma}}_{\boldsymbol{\xi}_j \boldsymbol{\xi}_j} = \widehat{\sigma}_\epsilon^2 (\mathbf{A}_j^\top \mathbf{A}_j)^{-1}$$

372 with

$$373 \quad (5.7) \quad \mathbf{A}_j = \left[\frac{\partial \widehat{\mathcal{Y}}(\mathbf{u}, \boldsymbol{\xi})}{\partial \boldsymbol{\xi}_j} \right]_{\substack{\boldsymbol{\xi}=\boldsymbol{\xi}^* \\ \mathbf{u}=\mathbf{U}_\mathcal{E}}} \in \mathbb{R}^{n_\mathcal{E} \times d} \quad \text{and} \quad \widehat{\sigma}_\epsilon^2 = \frac{1}{n_\mathcal{E} - md - P} \sum_{k=1}^{n_\mathcal{E}} [\mathbf{Y}_\mathcal{E}^k - \widehat{\mathcal{Y}}(\mathbf{U}_\mathcal{E}^k)]^2.$$

374 $\widehat{\sigma}_\epsilon^2$ is the standard estimator for the error variance of the surrogate model. \mathbf{A}_j is the gradient of the surrogate
 375 model \mathcal{Y} with respect to the model parameters evaluated at each of the $n_\mathcal{E}$ points in the training set $\mathbf{U}_\mathcal{E}$. \mathbf{A}_0
 376 is merely the design matrix and does not require the computation of any derivatives. Note that computing
 377 the gradients $\{\mathbf{A}_j\}_{j=0}^m$ does not require any model evaluations. For $j = 0$, it is

$$378 \quad (5.8) \quad \frac{\partial \widehat{\mathcal{Y}}(\mathbf{u}, \boldsymbol{\xi})}{\partial \boldsymbol{\xi}_0} = [\boldsymbol{\Psi}_i (\mathbf{W}^\top (\mathbf{u} - \boldsymbol{\mu}_\mathbf{U}))]_{i=1}^{P-1} \quad \text{with} \quad \mathbf{W} = [\boldsymbol{\xi}_1, \boldsymbol{\xi}_2, \dots, \boldsymbol{\xi}_m].$$

379 For $j > 0$ and recalling $\mathbf{z} = \mathbf{W}^\top(\mathbf{u} - \boldsymbol{\mu}_U)$, we have

$$\begin{aligned}
\frac{\partial \Psi_{\mathbf{k}}(\mathbf{z})}{\partial \xi_j} &= \frac{\partial}{\partial \mathbf{w}_j} \Psi_{\mathbf{k}}(\mathbf{W}^\top(\mathbf{u} - \boldsymbol{\mu}_U)) \\
&= (\mathbf{u} - \boldsymbol{\mu}_U) \frac{\partial \Psi_{\mathbf{k}}(z_j)}{\partial z_j} \\
380 \quad (5.9) \quad &= (\mathbf{u} - \boldsymbol{\mu}_U) \left(\prod_{\substack{i=1 \\ i \neq j}}^m \psi_{k_i}(\mathbf{w}_i^\top \mathbf{u}) \right) \frac{\partial \psi_{k_j}(\mathbf{w}_j^\top \mathbf{u})}{\partial z_j} \\
&= (\mathbf{u} - \boldsymbol{\mu}_U) \left(\prod_{\substack{i=1 \\ i \neq j}}^m \psi_{k_i}(\mathbf{w}_i^\top \mathbf{u}) \right) \sqrt{k_j} \psi_{k_j-1}(\mathbf{w}_j^\top \mathbf{u}).
\end{aligned}$$

381 In the last equality, we have used the following expression for derivatives of univariate normalized Hermite
382 polynomials:

$$383 \quad (5.10) \quad \frac{d\psi_n(x)}{dx} = \sqrt{n} \psi_{n-1}(x).$$

384 $\partial \widehat{\mathcal{Y}}(\mathbf{u}, \boldsymbol{\xi}) / \partial \xi_j$ for $j > 0$ follows as

$$385 \quad (5.11) \quad \frac{\partial \widehat{\mathcal{Y}}(\mathbf{u}, \boldsymbol{\xi})}{\partial \xi_j} = \frac{\partial \widehat{\mathcal{Y}}(\mathbf{z})}{\partial \mathbf{w}_j} = \sum_{\mathbf{k} \in \boldsymbol{\alpha}} \widehat{a}_{\mathbf{k}} \frac{\partial \Psi_{\mathbf{k}}(\mathbf{z})}{\partial \xi_j}, \quad j > 0.$$

386 The partial derivative $\partial \widehat{G} / \partial \xi_j$ in (5.5) can be evaluated using the chain rule of differentiation, which yields

$$387 \quad (5.12) \quad \frac{\partial \widehat{G}}{\partial \xi_j} = \frac{\partial \widehat{G}}{\partial \widehat{\mathcal{Y}}} \frac{\partial \widehat{\mathcal{Y}}}{\partial \xi_j}.$$

388 The first term on the right-hand side is typically easy to compute and often equals ± 1 (the sign is irrelevant
389 as the gradient enters the quadratic form in (5.5)) if the LSF returns the difference between the model out-
390 put and a prescribed threshold. In this case, the first factor on the right-hand side of (5.12) drops out. If,
391 however, the LSF is not continuously differentiable with respect to the model, we may construct a surrogate
392 model of G directly by using a training set containing LSF evaluations rather than model evaluations in
393 [Algorithm 4.1](#). The second term on the right-hand side can be obtained reusing the gradients from the \mathbf{A}_j
394 in (5.7) that — in this case — are not evaluated at the training set and thus are functions of \mathbf{u} .
395

396 When setting up the learning function, there is a distinction to be made between an intermediate SIS level
397 and the final SIS level: In the intermediate level, the goal is to accurately estimate the ratios of normalizing
398 constants and to propagate the samples to the next level. In the final level, the goal is to build the probability
399 of failure estimator and thus to accurately approximate the true limit-state hypersurface. With this in mind,
400 the learning functions for adapting the surrogate models in levels $i = 1, \dots, M$, and after the final level are
401 readily stated as

$$402 \quad (5.13) \quad \mathcal{L}_G(\mathbf{u}) = \begin{cases} \sigma_{\widehat{G}}(\mathbf{u}), & \text{intermediate SIS level} \\ \sigma_{\widehat{G}}(\mathbf{u}) / |\widehat{G}(\mathbf{u})|, & \text{after final SIS level.} \end{cases}$$

403 After the final level, SIS has converged and we are using samples from the final biasing density h_M to refit a
404 surrogate model that captures the failure hypersurface well. The learning function in this case is defined in
405 the spirit of the learning function put forward in [22]. The denominator penalizes samples whose image under
406 \widehat{G} is far away from 0 assuming that therefore they are themselves far away from the failure hypersurface.
407 Such samples are unlikely to be misclassified as safe if located in the failure domain or vice versa. In all
408 previous levels of SIS, there is no failure hypersurface to be approximated but only importance weights and

409 the resulting ratio of normalizing constants. Here, the denominator in the learning function is dropped as
 410 there is no benefit to penalizing samples with large absolute image values under \widehat{G} .

411

412 In each AL iteration, the pool is searched for one or several points maximizing $\mathcal{L}(\mathbf{u})$. If $n_{\text{add}} > 1$ new
 413 points are added per AL iteration, the current sample pool is transformed to the low-dimensional subspace
 414 defined by \mathbf{W} in order to identify n_{add} clusters (e.g., with k-means). Clustering in the subspace circum-
 415 vents the performance deterioration most clustering methods experience in high dimensions [40]. The point
 416 maximising (5.13) in each cluster is added to the training set. In this way, the algorithm avoids a local con-
 417 centration of the training set in a single region and is also able to handle problems with multiple disconnected
 418 failure domains as long as these are contained in the subspace.

419

420 The active learning is terminated based on the maximum local standard deviation relative to the target
 421 average in the intermediate levels or based on the relative change of the probability of failure estimate after
 422 the final level:

$$423 \quad (5.14) \quad \left\{ \begin{array}{ll} \max_{k=1, \dots, n} \left(\frac{\sigma_{\widehat{G}}(\mathbf{u}_k)}{\mathbb{E}[\widehat{G}(\mathcal{U})]} \right) \leq \epsilon_{\text{AL}}, & \text{intermediate SIS level} \\ \frac{\widehat{p} - \widehat{p}_{\text{last}}}{\widehat{p}} \leq \epsilon_{\text{AL}}, & \text{after final SIS level} \end{array} \right\},$$

424 where appropriate choices for ϵ_{AL} lie in $[10^{-2}, 10^{-1}]$. \widehat{p} and $\widehat{p}_{\text{last}}$ denote the probability of failure estimate
 425 based on the current and the last training set within the AL loop. The probability of failure is estimated
 426 with a surrogate model-based run of SIS-aCS in each AL iteration. This causes no additional cost in terms of
 427 original model evaluations and ensures a reliable evaluation of the criterion even for extremely small failure
 428 probabilities. The active learning procedure is detailed in Algorithm 5.1 and the complete method is detailed
 in Algorithm 5.2.

Algorithm 5.1 Active Learning

```

1: Input LSF  $G(\mathbf{u})$ , AL error level  $\epsilon_{\text{AL}}$ , # of AL clusters  $n_{\text{add}}$ , Polynomial order  $p$ , training set  $\{\mathbf{U}_{\mathcal{E}}, \mathbf{G}_{\mathcal{E}}\}$ ,
2:   Sample pool  $\mathbf{U}_{\text{pool}}$ 
3:
4: while true do ▷ Active learning loop
5:   Run  $[\mathbf{W}, \widehat{G}] = \text{PLS-PCE}(\mathbf{U}_{\mathcal{E}}, \mathbf{G}_{\mathcal{E}}, p, 'W')$  ▷ Algorithm 4.1
6:   if (5.14) then
7:     break
8:   Identify  $n_{\text{add}}$  clusters among  $\mathbf{U}_{\text{pool}}\mathbf{W}$  ▷ Clustering performed in the subspace defined by  $\mathbf{W}$ 
9:   for each cluster do
10:     $\mathbf{U}_{\text{cluster}} = \{\mathbf{u} \in \mathbf{U}_{\text{pool}} : \mathbf{u} \in \text{cluster}\}$ 
11:    Evaluate  $\mathbf{u}^* = \text{argmax}[\mathcal{L}(\mathbf{U}_{\text{cluster}})]$  according to (5.5)–(5.7), (5.12), and (5.13).
12:    Append  $\mathbf{U}_{\mathcal{E}} \leftarrow [\mathbf{U}_{\mathcal{E}}, \mathbf{u}^*]$ 
13:    Append  $\mathbf{G}_{\mathcal{E}} \leftarrow [\mathbf{G}_{\mathcal{E}}, G(\mathbf{u}^*)]$ 
14:    Remove  $\mathbf{u}^*$  from  $\mathbf{U}_{\text{pool}}$ 
15: return  $\mathbf{U}_{\mathcal{E}}, \mathbf{G}_{\mathcal{E}}, \widehat{G}$ .
```

429

430 6. Numerical experiments.

431 **6.1. Error measures.** In the following, we examine a series of examples of low to high input dimen-
 432 sionality characterized by varying degrees of nonlinearity of the LSF and varying number of disconnected
 433 failure regions. The computational cost of each approach is measured with the total number of required calls
 434 to the underlying computational model. The accuracy of the estimator is measured in terms of relative bias
 435 and CoV

$$436 \quad (6.1) \quad \text{relative Bias} = \frac{p - \mathbb{E}[\widehat{p}]}{p}$$

$$437 \quad (6.2) \quad \text{CoV} = \frac{\sqrt{\mathbb{V}[\widehat{p}]}}{\mathbb{E}[\widehat{p}]},$$

438

Algorithm 5.2 ASSIS (with PLS-PCE-W)

```

1: Input LSF  $G(\mathbf{u})$ , Target CoV  $\delta_{\text{target}}$ , Samples per level  $n$ , Input dimension  $d$ , training set size  $n_{\mathcal{E}}$ , AL
   error
2:     level  $\epsilon_{\text{AL}}$ , # of AL clusters  $n_{\text{add}}$ , Polynomial order  $p$ ,
3:
4: Set  $i = 0$ ,  $\sigma_i = \infty$ ,  $h_i(\mathbf{u}) = \varphi_d(\mathbf{u})$ 
5: Initialize  $\mathbf{U}_{\mathcal{E}} = [\cdot]$ ,  $\mathbf{G}_{\mathcal{E}} = [\cdot]$ 
6: Sample  $\mathbf{U}_0 = \{\mathbf{u}^k\}_{k=1}^{n_{\mathcal{E}}} \in \mathbb{R}^{n_{\mathcal{E}} \times d}$  ▷  $\mathbf{u}^k \stackrel{i.i.d.}{\sim} h_i(\mathbf{u})$ 
7: while true do ▷ Sequential importance sampling loop
8:   |  $i \leftarrow i + 1$ 
9:   | Sample  $\mathbf{U}_{\text{tmp}} = \{\mathbf{u}^k\}_{k=1}^{n_{\mathcal{E}}} \in \mathbb{R}^{n_{\mathcal{E}} \times d}$  ▷  $\mathbf{u}^k \stackrel{i.i.d.}{\sim} h_i(\mathbf{u})$ 
10:  | Compute  $\mathbf{G}_{\text{tmp}} = G(\mathbf{U}_{\text{tmp}}) \in \mathbb{R}^{n_{\mathcal{E}} \times 1}$ 
11:  | Append  $\mathbf{U}_{\mathcal{E}} \leftarrow [\mathbf{U}_{\mathcal{E}}, \mathbf{U}_{\text{tmp}}]$ 
12:  | Append  $\mathbf{G}_{\mathcal{E}} \leftarrow [\mathbf{G}_{\mathcal{E}}, \mathbf{G}_{\text{tmp}}]$ 
13:  | if  $i > 1$  then
14:  |   | Run  $\hat{G} = \text{PLS-PCE}(\mathbf{U}_{\mathcal{E}}, \mathbf{G}_{\mathcal{E}}, p, 'W')$  ▷ Algorithm 4.1
15:  |   | Run  $\mathbf{U}_{i-1}, \mathbf{G}_{i-1} = \text{SIS-aCS}(\hat{G}, \delta_{\text{target}}, n, d, i-1)$  ▷ Algorithm 3.1
16:  |   Run  $\mathbf{U}_{\mathcal{E}}, \mathbf{G}_{\mathcal{E}}, \hat{G} = \text{Active Learning}(G(\mathbf{u}), \epsilon_{\text{AL}}, n_{\text{add}}, p, \mathbf{U}_{\mathcal{E}}, \mathbf{G}_{\mathcal{E}}, \mathbf{U}_{i-1})$  ▷ Algorithm 5.1
17:  |   Compute  $\mathbf{G}_{i-1} = \hat{G}(\mathbf{U}_{i-1}) \in \mathbb{R}^{n_{\mathcal{E}} \times 1}$ 
18:  |   Compute  $\sigma_i$  according to (3.8)
19:  |   Compute  $\hat{\omega}_i$  and  $\hat{s}_i$  according to (5.2)
20:  |    $\mathbf{U}_{i-1}, \mathbf{G}_{i-1} \leftarrow \text{resample from } \mathbf{U}_{i-1}, \mathbf{G}_{i-1}$  with weights  $\hat{\omega}_i(\mathbf{U}_{i-1})$  ▷ sample with replacement
21:  |   Run  $\mathbf{U}_i, \mathbf{G}_i = \text{SIS-aCS}(\mathbf{U}_{i-1}, \mathbf{G}_{i-1})$  ▷ Perform a single MCMC step
22:  |   if (5.3) then
23:  |     | Set  $M \leftarrow i$ 
24:  |     | Run  $\mathbf{U}_{\mathcal{E}}, \mathbf{G}_{\mathcal{E}}, \hat{G} = \text{Active Learning}(G(\mathbf{u}), \epsilon_{\text{AL}}, n_{\text{add}}, p, \mathbf{U}_{\mathcal{E}}, \mathbf{G}_{\mathcal{E}}, \mathbf{U}_{i-1})$  ▷ Algorithm 5.1
25:  |     | break
26: Run  $(\mathbf{U}_M, \mathbf{G}_M, \hat{p}_{\text{ASSIS}}) = \text{SIS-aCS}(\hat{G}_M, \delta_{\text{target}}, n, d, M)$  ▷ Algorithm 3.1
27: return  $M, \mathbf{U}_M, \mathbf{G}_M, \hat{p}_{\text{ASSIS}}$ 

```

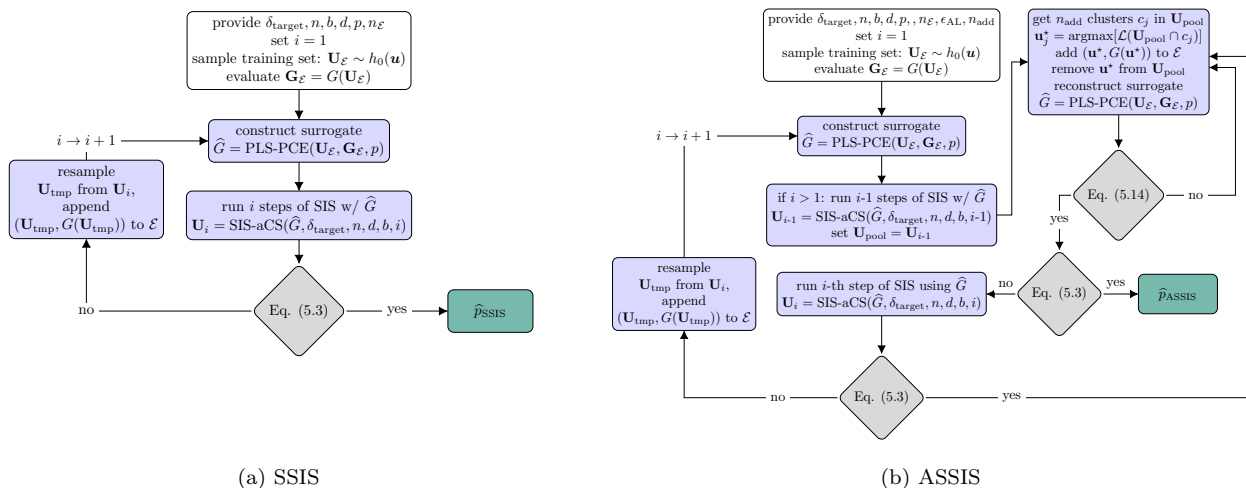


Fig. 3: Comparison of SIS-PLS-PCE with (right) and without (left) active learning.

Table 1: Low- to medium-dimensional investigated benchmark problems.

| Problem | Failure probability | Inputs | Input Variables | Properties | References |
|--|-----------------------|--------|------------------------|--|--------------------|
| Hat | $1.037 \cdot 10^{-4}$ | 2 | standard-normal | Strongly nonlinear | [70] |
| Cantilever | $3.94 \cdot 10^{-6}$ | 2 | Gaussian | Strongly nonlinear | [6] |
| 4-Branch (acc. to [6]) | $5.60 \cdot 10^{-9}$ | 2 | standard-normal | Multiple failure regions; extremely rare event | [6, 81] |
| Borehole ($276.7 \frac{m^3}{year}$) | $1 \cdot 10^{-5}$ | 8 | Log-normal, Uniform | Strongly nonlinear, No underlying low-dimensional structure | [1] |
| Truss (0.12m) | $1.6 \cdot 10^{-3}$ | 10 | Log-normal, Gumbel | mildly nonlinear | [43] |
| Rare Truss (0.18m) | $1.02 \cdot 10^{-8}$ | 10 | Log-normal, Gumbel | Extremely rare event; nonlinear | [43] (modified) |
| Quadratic ($\kappa = 5$) | $6.62 \cdot 10^{-6}$ | 10 | standard-normal | Strongly nonlinear; Underlying low-dimensional structure | [24, 80] |
| Quadratic ($\kappa = 5$) | $6.62 \cdot 10^{-6}$ | 100 | standard-normal | Strongly nonlinear; Underlying low-dimensional structure | [24, 80] |

439 where p is the known exact probability of failure or a reference solution computed with a large number of
 440 samples as reported in the corresponding references in Table 1. Further, we compute the relative root mean
 441 squared error (RMSE) of the probability of any failure estimate \hat{p} , which combines bias and variability of the
 442 estimator as

$$443 \quad (6.3) \quad \text{relative RMSE} = \sqrt{\frac{\mathbb{E}[(p - \hat{p})^2]}{p^2}} = \sqrt{\text{relative Bias}^2 + \left(\frac{\mathbb{E}[\hat{p}]}{p}\right)^2 \text{CoV}^2}$$

444 The expectation and variance operators in the above equations are approximated by repeating each analysis
 445 100 times. Additionally, the relative estimation error is defined as

$$446 \quad (6.4) \quad \text{relative error} = \frac{\hat{p}}{p}.$$

447 **6.2. Low- and medium-dimensional examples.** The subspace importance sampler is designed to
 448 tackle high-dimensional problems, yet its performance should not deteriorate as the problem dimension de-
 449 creases. We first investigate its performance in eight exemplary problems with dimension $2 \leq d \leq 100$.
 450 We demonstrate how both SSIS and ASSIS cope with multiple failure domains, strong nonlinearities and
 451 extremely small target failure probabilities. In the interest of brevity, the examples are listed in Table 1
 452 along with the problem dimension, target probability of failure and key characteristics of the problem. The
 453 references provided in Table 1 may be consulted for detailed descriptions of the problem setups.

454 We solve the example problems with SIS-aCS with $n = 2 \cdot 10^3$ samples per level and a burn-in period
 455 of $b = 5$ samples within each MCMC chain. As suggested in [61], we choose $\delta_{\text{target}} = 1.5$ for the exit criterion
 456 (3.9) for SIS-aCS as well as our surrogate-based samplers. We compare this reference to SSIS and ASSIS
 457 for which we use an initial sample size of $n_{\mathcal{E}} = 5d$. All underlying PLS-PCE-W models are computed with
 458 a maximum number of subspace directions of $m = 10$ and a maximum total polynomial degree of $|q|_{\ell_q} \leq 7$,
 459 where $q = 0.75$. To achieve a fair comparison between ASSIS and SSIS, we first run ASSIS and then SSIS
 460 with $n_{\mathcal{E}}$ for the latter chosen such that both methods use an approximately equal number of LSF evaluations.
 461 For both SSIS and ASSIS, we choose $n = 10^4$ with a burn-in period of $b = 30$. For ASSIS, we set $\epsilon_{\text{AL}} = 0.1$.

463 Within SSIS/ASSIS many samples per level and long burn-in periods are affordable as sampling is performed
 464 with the surrogate model. For ASSIS we select $n_{\text{add}} = 1$ unless prior knowledge of the problem structure
 465 suggests otherwise (the only exception in the set of examples considered here is the 4-branch function for
 466 which we select $n_{\text{add}} = 4$ as it features four relevant failure regions in the input space). Fig. 4 displays the
 467 performance of SIS, SSIS and ASSIS for the examples in Table 1 in terms of the error measures defined in
 (6.1)–(6.3) and the total number of LSF evaluations (with the original model).

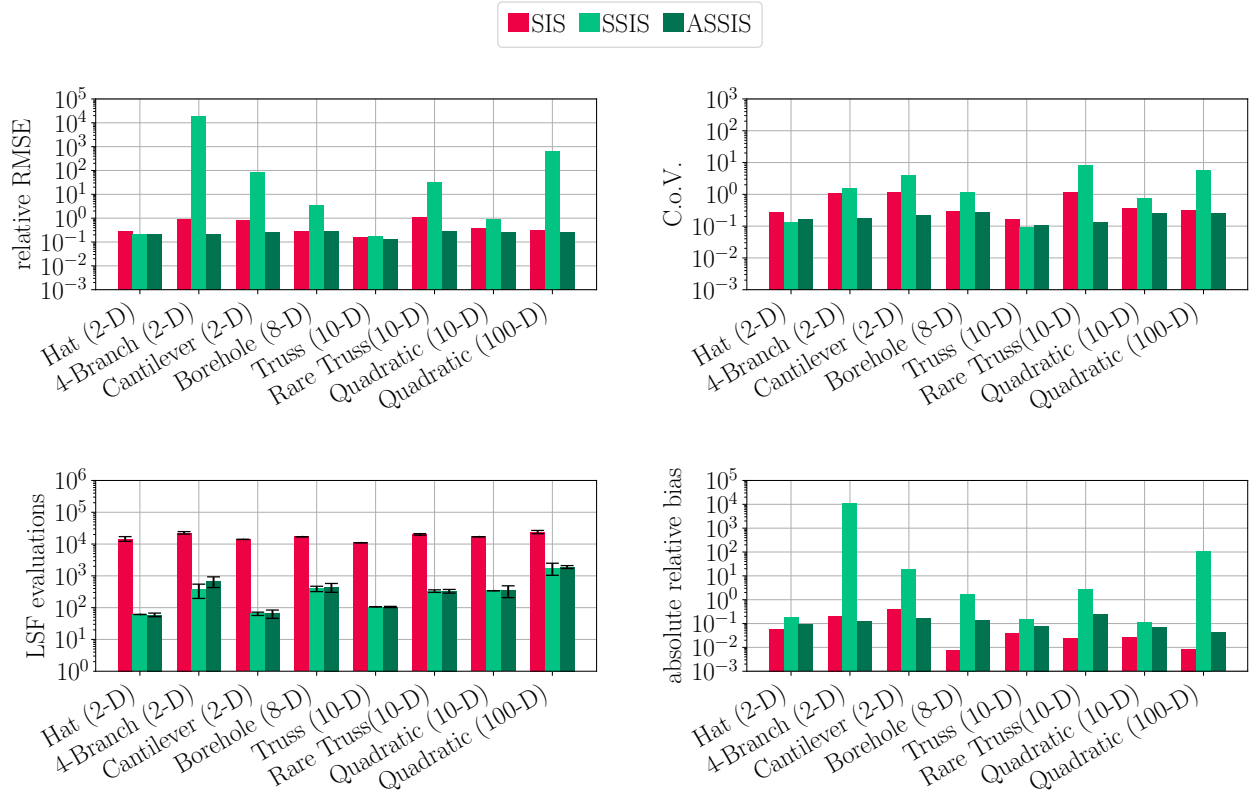


Fig. 4: Low- and medium-dimensional examples: accuracy and cost comparison. Cost error bars include ± 2 standard deviations.

468

469

470 For all showcased examples, ASSIS yields equally or more accurate estimates compared to SSIS at equal cost.
 471 It also either matches or outperforms SIS at significantly reduced costs. Except for the easiest problems,
 472 i.e., those featuring well-behaved (truss) or low-dimensional (2D hat) LSFs associated with comparatively
 473 large failure probabilities, the in-level adaptivity of ASSIS leads to significant bias correction (Fig. 4, bottom
 474 right) and variance reduction (Fig. 4, top right).

475

476 [61] discusses the choice of the MCMC sampler for SIS and find that aCS as employed here is outper-
 477 formed by a Gaussian mixture proposal in low-dimensional problems, while the latter is the preferred choice
 478 as the problem dimension grows. Our method is designed for the solution of high-dimensional reliability
 479 problems and we thus consistently use aCS.

480

481 Comparing the truss and the rare truss models, the additional number of SIS levels required in the solu-
 482 tion of the latter evidently leads to a deterioration of the SSIS estimate (Fig. 4, top left). This is due to
 483 single runs (less than 10 %) among the 100 repetitions in which the sampled training sets lead to extreme
 484 outliers in the failure probability estimates (Fig. 5). While this effect vanishes when increasing the number
 485 of samples in the training set, ASSIS offers a more cost-effective alternative to avoid such outliers by actively

486 learning an informative augmentation of adverse training sets. In this way, subspace identification and surro-
 487 gate modelling errors cannot propagate and accumulate across the levels of SIS as they are controlled by the
 488 AL procedure. In fact, the phenomenon of rather rare but all the more severe outliers deteriorating the error
 489 mean and variability is a problem SSIS is facing not only in the rare truss example but also in the cantilever
 490 and both quadratic examples. Conversely, it is seen that in the 4-branch example, SSIS consistently and
 491 considerably overestimates the probability of failure while ASSIS captures the probability of failure rather
 492 well.
 493

The two quadratic LSF models with 10 and 100 input dimensions demonstrate how the required num-

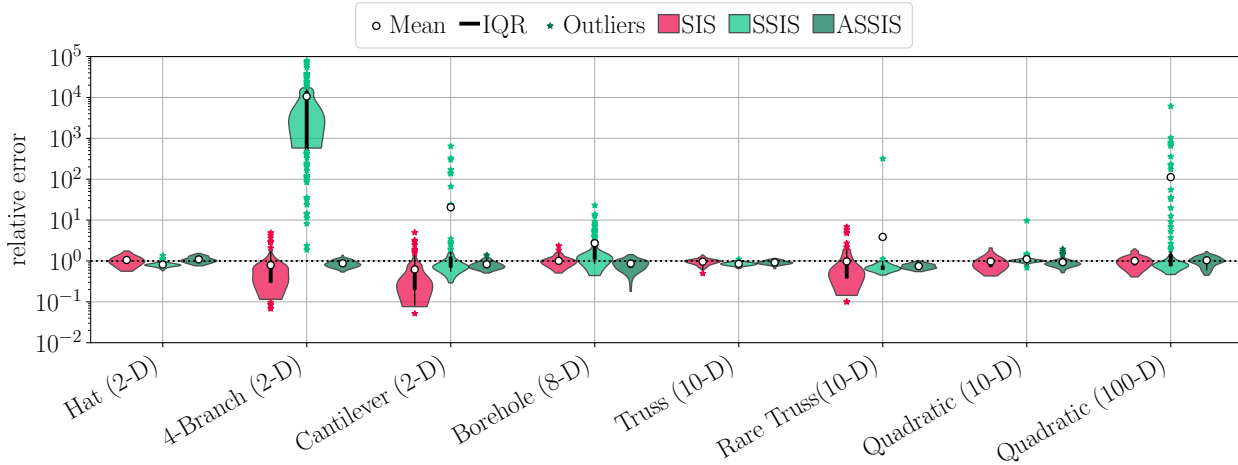


Fig. 5: Low- and medium-dimensional examples: violin plots of the relative error along with means, inter-quartile ranges (IQR) and outliers. For the sake of clarity, kernel density estimates are computed after excluding outliers based on the relative distance to the data median.

494
 495 ber of LSF evaluations depends on the problem dimension in both surrogate-based approaches. This is due
 496 to the fact that the PLS-PCE model requires at least d (often more) samples to identify a suitable subspace.
 497 Thus, as described above, we choose $n_{\mathcal{E}}$ as a multiple of d . Since the surrogate-free version of SIS-aCS does
 498 not possess such a dependence on a problem dimension at all, the ratio of computational cost associated
 499 with SIS and ASSIS decreases as d increases. This observation also indicates that if d grows large enough,
 500 SIS-aCS will outperform any surrogate-based approach. This is expected for cases with $d = \mathcal{O}(10^5)$ and
 501 above; therefore, this observation is of little practical relevance for most engineering models, where ASSIS
 502 will likely be the most cost-effective choice.

503 **6.3. High-dimensional example: Steel plate.** We consider a modified version of the example given
 504 in [80, 49], which consists of a low-carbon steel plate of length 0.32 m, width 0.32 m, thickness $t = 0.01$ m,
 505 and a hole of radius 0.02 m located at the center. The Poisson ratio is set to $\nu = 0.29$ and the density of the
 506 plate is $\rho = 7850$ kg/m³. The horizontal and vertical displacements are constrained at the left edge. The
 507 plate is subjected to a random surface load that acts on the right narrow plate side. The load is modelled as
 508 a log-normal random variable with mean $\mu_q = 60$ MPa and $\sigma_q = 12$ MPa. The Young's modulus $E(x, y)$ is
 509 considered uncertain and spatially variable. It is described by a homogeneous random field with lognormal
 510 marginal distribution, mean value $\mu_E = 2 \times 10^5$ MPa and standard deviation $\sigma_E = 3 \times 10^4$ MPa. The
 511 autocorrelation function of the underlying Gaussian field $\ln E$ is modeled by the isotropic exponential model

512 (6.5)
$$\rho_{\ln E}(\Delta x, \Delta y) = \exp \left\{ -\frac{\sqrt{\Delta x^2 + \Delta y^2}}{l_E} \right\}$$

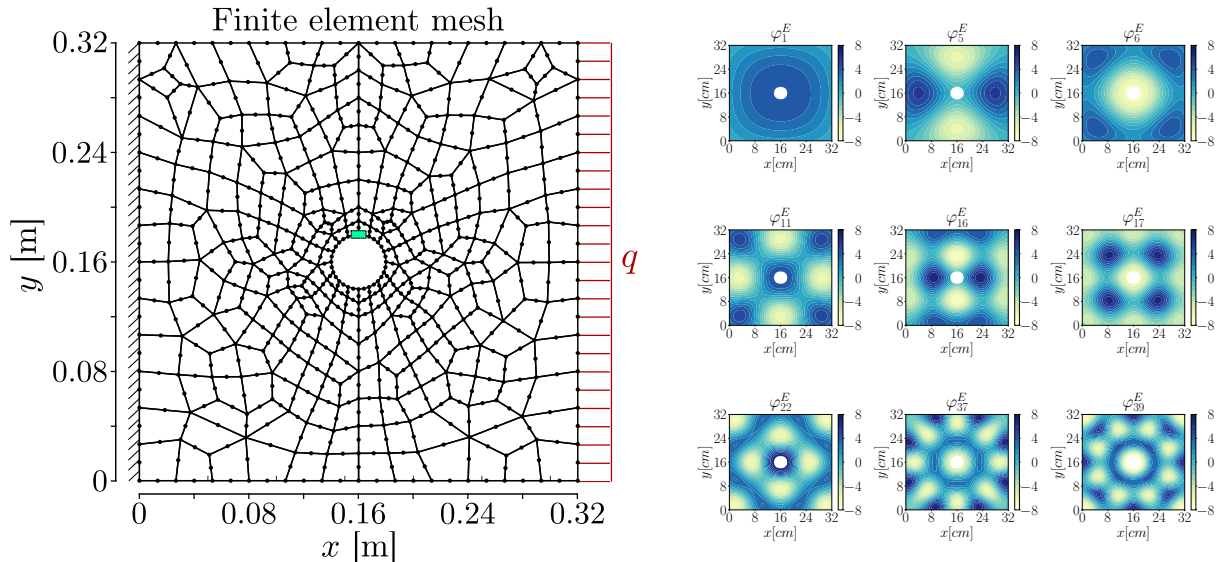


Fig. 6: Left: FE-mesh of 2D-plate model with control node of the first principal stress σ_1 .

513 with correlation length $l_{\ln E} = 0.04\text{m}$. The Gaussian random field $\ln E$ is discretized by a Karhunen-Loève-
 514 expansion (KLE) with $d_E = 868$, which yields a mean error variance of 7.5% and reads

$$515 \quad (6.6) \quad E(x, y) = \exp \left\{ \mu_{\ln E} + \sigma_{\ln E} \sum_{i=1}^{d_E} \sqrt{\lambda_i^E} \varphi_i^E(x, y) \xi_i \right\}.$$

516 $\mu_{\ln E}$ and $\sigma_{\ln E}$ are the parameters of the log-normal marginal distribution of E , $\{\lambda_i^E, \varphi_i^E\}$ are the eigenpairs
 517 of the correlation kernel in (6.5) and $\boldsymbol{\xi} \in \mathbb{R}^{d \times 1}$ is a standard-normal random vector. The most influential
 518 eigenfunctions (based on a global output-oriented sensitivity analysis of the plate model performed in [23])
 519 are shown in Fig. 6 on the right.

520

521 The stress ($\boldsymbol{\sigma}(x, y) = [\sigma_x(x, y), \sigma_y(x, y), \tau_{xy}(x, y)]^T$), strain ($\boldsymbol{\epsilon}(x, y) = [\epsilon_x(x, y), \epsilon_y(x, y), \gamma_{xy}(x, y)]^T$) and dis-
 522 placement ($\mathbf{u}(x, y) = [u_x(x, y), u_y(x, y)]^T$) fields of the plate are given through elasticity theory, namely the
 523 Cauchy-Navier equations [37]. Given the configuration of the plate, the model can be simplified under the
 524 plane stress hypothesis, which yields

$$525 \quad (6.7) \quad G(x, y) \nabla^2 \mathbf{u}(x, y) + \frac{E(x, y)}{2(1-\nu)} \nabla(\nabla \cdot \mathbf{u}(x, y)) + \mathbf{b} = 0.$$

Therein, $G(x, y) := E(x, y)/(2(1 + \nu))$ is the shear modulus, and $\mathbf{b} = [b_x, b_y]^T$ is the vector of body forces acting on the plate. (6.7) is discretized with a finite-element method. That is, the spatial domain of the plate is discretized into 282 eight-noded quadrilateral elements, as shown in Fig. 6. In a grid independence study, the plate's probability of failure was found to slightly increase with decreasing mesh element size, which is likely due to the reduction of averaging effects when integrating higher-order KL-terms. However, for the purpose of testing ASSIS, the model is sufficiently accurate and features two important properties: 1. It possesses a low-dimensional structure that can be exploited with dimensionality-reducing surrogates. 2. It is truly high-dimensional in the sense that the solution does not only depend on a small subset of the input variables (i.e., the low-dimensional structure is not a trivial subspace of the original input space). The LSF is defined by means of a threshold for the the first principal plane stress

$$\sigma_1 = 0.5(\sigma_x + \sigma_y) + \sqrt{[0.5(\sigma_x + \sigma_y)]^2 + \tau_{xy}^2}$$

Table 2: Accuracy and cost of SIS, SSIS & ASSIS for the plate example based on 100 repetitions of the analysis. The reference $p_{\text{ref}} = 4.23 \cdot 10^{-6}$ is computed with 100 repeated runs of subset simulation with 10^4 samples per level with $\text{CoV} = 0.0119$ for the mean estimate.

| Method | $\mathbb{E}[p]$ | relative RMSE | CoV | relative bias | avg. # LSF evaluations |
|---------|----------------------|---------------|-------|---------------|------------------------|
| SIS-aCS | $3.88 \cdot 10^{-6}$ | 0.576 | 0.625 | 0.083 | 17000 |
| SSIS | $3.99 \cdot 10^{-6}$ | 0.061 | 0.021 | 0.058 | 1300 |
| ASSIS | $4.10 \cdot 10^{-6}$ | 0.036 | 0.021 | 0.030 | 1318 |

526 evaluated at node 11 (see green marker Fig. 6, left). Node 11 indicates a location where maximum plane
 527 stresses occur frequently in this example. The LSF reads

$$528 \quad (6.8) \quad g(\mathbf{U}) = \sigma_{\text{threshold}} - \sigma_1(\mathbf{U}),$$

529 where $\sigma_{\text{threshold}} = 450$ MPa. The target probability of failure is determined to $p = 4.23 \cdot 10^{-6}$ with
 530 $\text{CoV} = 0.0119$ as the average of 100 repeated runs of subset simulation [3] with 10^4 samples per level.

531
 532 SIS-aCS is run with $n = 2 \cdot 10^3$ samples per level and a burn-in period of $b = 5$ samples within each
 533 MCMC chain. SSIS and ASSIS are run with $n = 10^5$ samples per SIS level, a burn-in period $b = 30$ and an
 534 AL threshold of $\epsilon_{\text{AL}} = 0.1$. In the first level $n_{\mathcal{E}} = 900$ and in each additional level only $n_{\mathcal{E}} = 100$ samples
 535 are added in the initial sampling phase. Table 2 lists the average estimated probabilities of failure along
 536 with error measures and average number of required LSF evaluations. It is seen that both SSIS and ASSIS
 537 alleviate computational cost by more than an order of magnitude while at the same time reducing the relative
 538 RMSE by at least an order of magnitude. The decomposition of the RMSE in CoV and relative bias reveals
 539 that this is mostly due to variance reduction as SIS-aCS already yields a small bias.

540
 541 A parameter study of important 'tweakable' parameters of ASSIS is depicted in Fig. 7. Parameters that are
 542 not subject to a parametric study are chosen as above, with the exception of $n = 10^4$ instead of $n = 10^5$.
 543 The estimation error and computational cost of ASSIS is analyzed for varying active learning threshold ϵ_{AL} ,
 544 number of samples in the training set $n_{\mathcal{E}}$, the number of samples per SIS level n and the target CoV δ_{target}
 545 used for the SIS procedure. The scaling of 10% between the initial training set and all subsequent training
 546 samples is kept constant.

547
 548 The parameters ϵ_{AL} and $n_{\mathcal{E}}$ describe the behaviour of the surrogate modelling and active learning pro-
 549 cedures while n and δ_{target} describe SIS itself. Fig. 7 shows that increasing the target coefficient of variation
 550 leads to a reduced number of levels in the SIS procedure, which is directly associated with a reduction in
 551 computational cost. The reduction is relatively small here as most of the samples are added in the first level.
 552 By design, the number of required samples remains unaffected by varying the number of samples per SIS level,
 553 while the estimation error depends reciprocally on it. Conversely, and also by design, the computational cost
 554 depends monotonically on the choice of $n_{\mathcal{E}}$. If a majority of the used original LSF evaluations are added dur-
 555 ing an AL procedure, this relationship may be nonlinear. For the plate example, however, the initially drawn
 556 training samples at each level makes up for the majority of used original LSF evaluations, hence the linear
 557 dependency. The estimation errors decrease slightly with increasing training set size, although the effect is
 558 limited as high accuracy is already achieved with the first training set of the lowest investigated size. The fact
 559 that the subspace does not change significantly with increasing SIS level leaves little to be learned by adding
 560 more LSF evaluations to the training set. This is also the reason for the competitive performance of SSIS
 561 in this example. The estimation errors (as well as the computational cost in this case) remain unaffected by
 562 varying AL thresholds ϵ_{AL} , which is in line with the observation that a large fraction of the computational
 563 budget is spent on sampling the initial training set rather than the AL-based training set augmentation.

564 **7. Concluding remarks.** This paper proposes a method for the cost-efficient solution of high-dimensional
 565 reliability problems. We build on a recently introduced dimensionality reducing surrogate modelling tech-
 566 nique termed partial least squares-driven polynomial chaos expansion (PLS-PCE) [59] and previous work, in

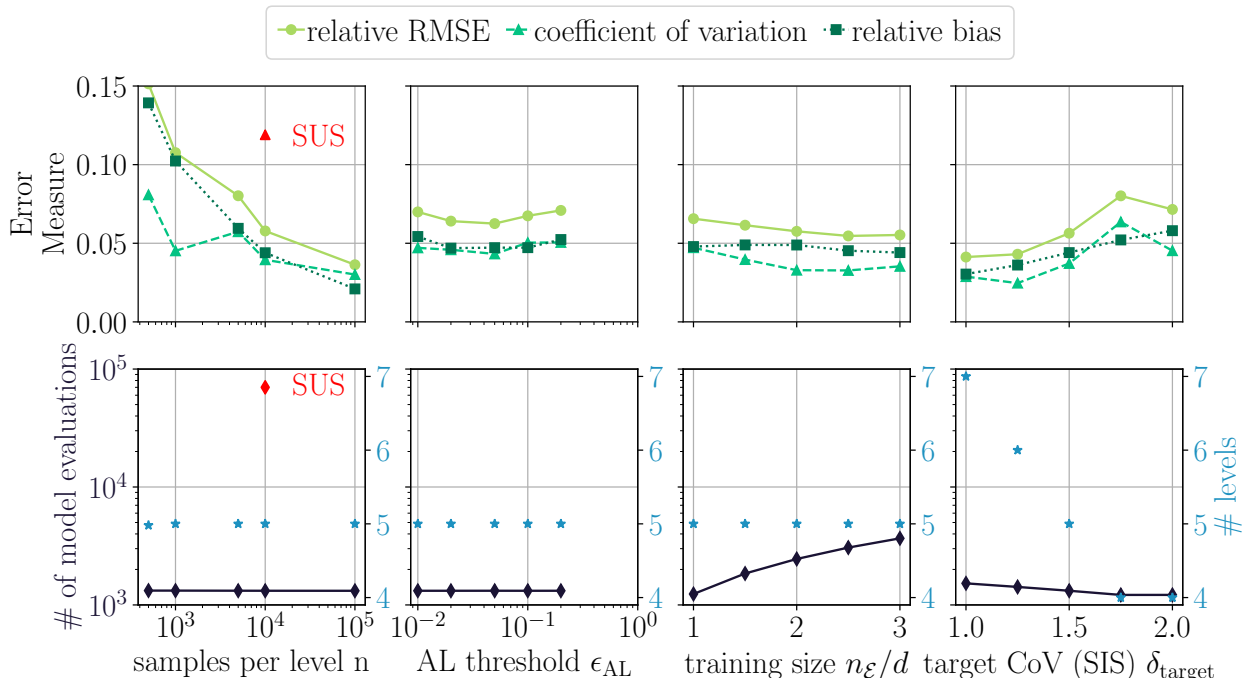


Fig. 7: Steel plate reliability using ASSIS: parameter influence studies. Top: Error measures as defined in (6.1)–(6.3) for ASSIS (green lines w/ markers). Bottom: Computational cost in terms of total number of limit-state function evaluations with the true computational model (left y-axis; black solid lines with diamond markers) and number of SIS levels to convergence (right y-axis; blue star markers). Top left: CoV of a subset simulation reference run with $n = 10^4$ samples per level (red triangle marker). Bottom left: total number of required limit-state function evaluations of a subset simulation reference run with $n = 10^4$ samples per level (red triangle marker).

567 which we use PLS-PCE surrogates to reconstruct biasing densities within a sequential importance sampling
 568 scheme [58] (sequential subspace importance sampling: SSIS). We refine this approach by devising an active
 569 learning procedure in each SIS level, which serves to effectively control the estimation error introduced by
 570 the surrogate-based importance density reconstructions. The learning procedure, i.e., the selection of new
 571 points for the training set, is driven by an estimate of both the subspace and surrogate model estimation
 572 error. This criterion can be generally used in polynomial chaos expansion-based active learning procedures.
 573

574 We showcase the performance of SSIS and ASSIS in nine example applications with input dimensional-
 575 ity ranging from $d = 2$ to 869. The examples feature different typical caveats for reliability methods such as
 576 multiple failure domains, strongly nonlinear limit-state functions and extremely small target probabilities of
 577 failure. Depending on the example, we achieve a cost reduction of one to over two orders of magnitude with
 578 ASSIS compared to the reference method (sequential importance sampling with the original model) at equal
 579 or lower estimation errors. It is shown that SSIS is susceptible to the randomness of the initial training set
 580 occasionally producing outliers if the training set is adverse. The active learning procedure (ASSIS) remedies
 581 this drawback and stabilizes the estimator by augmenting potentially adverse training sets with informative
 582 additional samples.
 583

584 The million dollar question, as with any surrogate model, is on the method's ability to generalize. Certainly,
 585 there exist examples that do not possess a suitable linear subspace as required by PLS-PCE modelling.
 586 Further, cases of model misspecification may arise if the computational model cannot be represented with
 587 PCEs (e.g., if it is a rational function). Then, the probability of failure estimate produced by ASSIS will
 588 be neither consistent nor unbiased. However, by means of coupling PLS-PCE with sequential importance

589 sampling, both requirements are relaxed somewhat as only a locally accurate surrogate model is required to
 590 propagate samples from one intermediate biasing density to the next. Hence, ASSIS can still be expected to
 591 perform well if the computational model may be represented in terms of a sequence of local linear subspaces
 592 on which the model can be approximated well with polynomials. Relaxing the orthogonality or even the
 593 linearity assumption on the latent space transformation likely bears potential to improve the performance
 594 of dimensionality-reduced PCEs. Doing so will require methods to track the appropriate PCE basis upon
 595 determining the law of the transformed input random vector (as these will not be standard-normal if the
 596 latent space transformation is no longer subject to the orthogonality constraint).

597 **8. Acknowledgment.** This project was supported by the German Research Foundation (DFG) through
 598 Grant STR 1140/6-1 under SPP 1886.

599 REFERENCES

600 [1] J. AN AND A. OWEN, *Quasi-regression*, Journal of Complexity, 17 (2001), pp. 588 – 607.
 601 [2] S. AU AND J. BECK, *A new adaptive importance sampling scheme for reliability calculations*, Structural Safety, 21 (1999),
 602 pp. 135 – 158.
 603 [3] S.-K. AU AND J. L. BECK, *Estimation of small failure probabilities in high dimensions by subset simulation*, Probabilistic
 604 Engineering Mechanics, 16 (2001), pp. 263–277, [https://doi.org/10.1016/S0266-8920\(01\)00019-4](https://doi.org/10.1016/S0266-8920(01)00019-4),
 605 <https://www.sciencedirect.com/science/article/pii/S0266892001000194>.
 606 [4] G. BAFFI, E. MARTIN, AND A. MORRIS, *Non-linear projection to latent structures revisited (the neural network PLS
 607 algorithm)*, Computers & Chemical Engineering, 23 (1999), pp. 1293–1307.
 608 [5] M. BALESDENT, J. MORIO, AND J. MARZAT, *Kriging-based adaptive importance sampling algorithms for rare event es-
 609 timation*, Structural Safety, 44 (2013), pp. 1 – 10, <https://doi.org/10.1016/j.strusafe.2013.04.001>,
 610 <http://www.sciencedirect.com/science/article/pii/S0167473013000350>.
 611 [6] J. BECT, L. LI, AND E. VAZQUEZ, *Bayesian subset simulation*, SIAM/ASA Journal on Uncertainty Quantification, 5
 612 (2017), pp. 762–786, <https://doi.org/10.1137/16M1078276>, <https://doi.org/10.1137/16M1078276>, [https://arxiv.org/
 613 abs/https://doi.org/10.1137/16M1078276](https://arxiv.org/abs/https://doi.org/10.1137/16M1078276).
 614 [7] M. BERVEILLER, B. SUDRET, AND M. LEMAIRE, *Stochastic finite element: a non intrusive approach by regression*, European
 615 Journal of Computational Mechanics, 15 (2006), pp. 81–92.
 616 [8] B. J. BICHON, M. S. ELDERED, L. P. SWILER, S. MAHADEVAN, AND J. M. MCFARLAND, *Efficient global reliability analysis for
 617 nonlinear implicit performance functions*, AIAA Journal, 46 (2008), pp. 2459–2468, <https://doi.org/10.2514/1.34321>,
 618 <https://doi.org/10.2514/1.34321>, <https://arxiv.org/abs/https://doi.org/10.2514/1.34321>.
 619 [9] G. BLATMAN AND B. SUDRET, *Sparse polynomial chaos expansions and adaptive stochastic finite elements using a regression
 620 approach*, Comptes Rendus Mécanique, 336 (2008), pp. 518–523, [https://doi.org/10.1016/j.crme.2008.
 621 02.013](https://doi.org/10.1016/j.crme.2008.02.013), <https://www.sciencedirect.com/science/article/pii/S1631072108000582>.
 622 [10] G. BLATMAN AND B. SUDRET, *Adaptive sparse polynomial chaos expansion based on least-angle regression*, Journal of
 623 Computational Physics, 230 (2011), pp. 2345 – 2367, <https://doi.org/10.1016/j.jcp.2010.12.021>.
 624 [11] J.-M. BOURINET, *Rare-event probability estimation with adaptive support vector regression surrogates*, Reliability En-
 625 gineering & System Safety, 150 (2016), pp. 210 – 221, <https://doi.org/10.1016/j.res.2016.01.023>,
 626 <http://www.sciencedirect.com/science/article/pii/S0951832016000387>.
 627 [12] J.-M. BOURINET, F. DEHEEGER, AND M. LEMAIRE, *Assessing small failure probabilities by combined subset simulation
 628 and support vector machines*, Structural Safety, 33 (2011), pp. 343 – 353, [https://doi.org/http://dx.doi.org/10.1016/
 629 j.strusafe.2011.06.001](https://doi.org/http://dx.doi.org/10.1016/j.strusafe.2011.06.001), <http://www.sciencedirect.com/science/article/pii/S0167473011000555>.
 630 [13] C. G. BUCHER, *Adaptive sampling — an iterative fast Monte Carlo procedure*, Structural Safety, 5 (1988), pp. 119 – 126.
 631 [14] F. CADINI, F. SANTOS, AND E. ZIO, *An improved adaptive kriging-based importance technique for sampling multiple failure
 632 regions of low probability*, Reliability Engineering & System Safety, 131 (2014), pp. 109 – 117, <https://doi.org/https://doi.org/10.1016/j.res.2014.06.023>,
 633 <http://www.sciencedirect.com/science/article/pii/S0951832014001537>.
 634 [15] O. CHAPPELLE, V. VAPNIK, AND Y. BENGIO, *Model selection for small sample regression*, Machine Learning, 48 (2002),
 635 pp. 9–23.
 636 [16] P. G. CONSTANTINE, E. DOW, AND Q. WANG, *Active subspace methods in theory and practice: Applications to Kriging
 637 surfaces*, SIAM Journal on Scientific Computing, 36 (2014), pp. A1500–A1524, <https://doi.org/10.1137/130916138>.
 638 [17] S. DE JONG, *Pls shrinks*, Journal of Chemometrics, 9 (1995), pp. 323–326, [https://doi.org/https://doi.org/10.1002/cem.
 639 1180090406](https://doi.org/https://doi.org/10.1002/cem.1180090406).
 640 [18] A. DER KIUREGHIAN, *First-and second-order reliability methods*, in Engineering Design Reliability Handbook, E. Nikolaidis,
 641 D. M. Ghiocel, and S. Singhal, eds., CRC Press, Boca Raton, FL, 2005, ch. 14.
 642 [19] O. DITLEVSEN AND H. O. MADSEN, *Structural reliability methods*, John Wiley & Sons Ltd, 1996.
 643 [20] A. DOOSTAN AND H. OWHADI, *A non-adapted sparse approximation of PDEs with stochastic inputs*, Journal of Computa-
 644 tional Physics, 230 (2011), pp. 3015–3034.
 645 [21] V. DUBOURG, B. SUDRET, AND F. DEHEEGER, *Metamodel-based importance sampling for structural reliability analysis*,
 646 Probabilistic Engineering Mechanics, 33 (2013), pp. 47 – 57, [https://doi.org/http://dx.doi.org/10.1016/j.probengmech.
 647 2013.02.002](https://doi.org/http://dx.doi.org/10.1016/j.probengmech.2013.02.002), <http://www.sciencedirect.com/science/article/pii/S0266892013000222>.
 648 [22] B. ECHARD, N. GAYTON, AND M. LEMAIRE, *AK-MCS: An active learning reliability method combining Kriging and Monte
 649 Carlo simulation*, Structural Safety, 33 (2011), pp. 145 – 154, [https://doi.org/http://dx.doi.org/10.1016/j.strusafe.
 650 2011.01.002](https://doi.org/http://dx.doi.org/10.1016/j.strusafe.2011.01.002), <http://www.sciencedirect.com/science/article/pii/S0167473011000038>.

- 651 [23] M. EHRE, I. PAPAIOANNOU, AND D. STRAUB, *Global sensitivity analysis in high dimensions with PLS-PCE*, Reliability
652 Engineering & System Safety, 198 (2020), p. 106861, <https://doi.org/https://doi.org/10.1016/j.res.2020.106861>, <http://www.sciencedirect.com/science/article/pii/S0951832019314140>.
- 653 [24] S. ENGELUND AND R. RACKWITZ, *A benchmark study on importance sampling techniques in structural reliability*, Structural
654 Safety, 12 (1993), pp. 255 – 276.
- 655 [25] L. FARAVELLI, *Response surface approach for reliability analysis*, Journal of Engineering Mechanics, 115 (1989),
656 pp. 2763–2781, [https://doi.org/10.1061/\(ASCE\)0733-9399\(1989\)115:12\(2763\)](https://doi.org/10.1061/(ASCE)0733-9399(1989)115:12(2763)), <http://ascelibrary.org/doi/abs/10.1061/%28ASCE%290733-9399%281989%29115%3A12%282763%29>.
- 657 [26] V. FEDOROV, *Theory of Optimal Experiments*, Probability and Mathematical Statistics, Academic Press, 01 1972, <https://books.google.de/books?id=PpUIwgEACAAJ>.
- 660 [27] B. FIESSLER, R. RACKWITZ, AND H.-J. NEUMANN, *Quadratic limit states in structural reliability*, Journal of the Engineering
661 Mechanics Division, 105 (1979), pp. 661–676.
- 662 [28] X. GUAN AND R. MELCHERS, *Effect of response surface parameter variation on structural reliability estimates*, Structural
663 Safety, 23 (2001), pp. 429 – 444, [https://doi.org/http://dx.doi.org/10.1016/S0167-4730\(02\)00013-9](https://doi.org/http://dx.doi.org/10.1016/S0167-4730(02)00013-9), <http://www.sciencedirect.com/science/article/pii/S0167473002000139>.
- 664 [29] M. HOHENBICHLER AND R. RACKWITZ, *Non-normal dependent vectors in structural safety*, Journal of the Engineering
665 Mechanics Division, 107 (1981), pp. 1227–1238.
- 666 [30] M. HOHENBICHLER AND R. RACKWITZ, *Improvement of second-order reliability estimates by importance sampling*, Journal
667 of Engineering Mechanics, 114 (1988), pp. 2195–2199.
- 668 [31] A. HÖSKULDSSON, *PLS regression methods*, Journal of Chemometrics, 2 (1988), pp. 211–228.
- 669 [32] X. HUANG, J. CHEN, AND H. ZHU, *Assessing small failure probabilities by AK-SS: An active learning method combining
670 Kriging and subset simulation*, Structural Safety, 59 (2016), pp. 86 – 95, <https://doi.org/https://doi.org/10.1016/j.strusafe.2015.12.003>, <http://www.sciencedirect.com/science/article/pii/S0167473016000035>.
- 671 [33] J. E. HURTADO, *Filtered importance sampling with support vector margin: a powerful method for structural reliability
672 analysis*, Structural Safety, 29 (2007), pp. 2–15.
- 673 [34] J. E. HURTADO AND D. A. ALVAREZ, *Neural-network-based reliability analysis: a comparative study*, Computer Methods
674 in Applied Mechanics and Engineering, 191 (2001), pp. 113–132.
- 675 [35] S. JI, Y. XUE, AND L. CARIN, *Bayesian compressive sensing*, IEEE Transactions on Signal Processing, 56 (2008), pp. 2346–
676 2356.
- 677 [36] Z. JIANG AND J. LI, *High dimensional structural reliability with dimension reduction*, Structural Safety, 69 (2017), pp. 35 –
678 46, <https://doi.org/https://doi.org/10.1016/j.strusafe.2017.07.007>, <http://www.sciencedirect.com/science/article/pii/S0167473016302077>.
- 681 [37] C. JOHNSON, *Numerical solution of partial differential equations by the finite element method*, Dover Publications, 2009.
- 682 [38] K. KONAKLI AND B. SUDRET, *Reliability analysis of high-dimensional models using low-rank tensor approximations*, Prob-
683 abilistic Engineering Mechanics, 46 (2016), pp. 18 – 36.
- 684 [39] P. KOUTSOURELAKIS, H. PRADLWARTER, AND G. SCHUËLLER, *Reliability of structures in high dimensions, part I: algorithms
685 and applications*, Probabilistic Engineering Mechanics, 19 (2004), pp. 409 – 417.
- 686 [40] H. KRIEGEL, P. KRÖGER, AND A. ZIMEK, *Clustering high-dimensional data: A survey on subspace clustering, pattern-based
687 clustering, and correlation clustering*, ACM Trans. Knowl. Discov. Data, 3 (2009), pp. 1:1–1:58.
- 688 [41] D. P. KROESE, R. Y. RUBINSTEIN, AND P. W. GLYNN, *Chapter 2 - The cross-entropy method for estimation*, in Handbook
689 of Statistics: Machine Learning: Theory and Applications, vol. 31 of Handbook of Statistics, Elsevier, 2013, pp. 19 –
690 34.
- 691 [42] N. KURTZ AND J. SONG, *Cross-entropy-based adaptive importance sampling using Gaussian mixture*, Structural Safety, 42
692 (2013), pp. 35 – 44.
- 693 [43] S. H. LEE AND B. M. KWAK, *Response surface augmented moment method for efficient reliability analysis*, Structural
694 Safety, 28 (2006), pp. 261 – 272.
- 695 [44] J. LI, J. LI, AND D. XIU, *An efficient surrogate-based method for computing rare failure probability*, Journal of
696 Computational Physics, 230 (2011), pp. 8683 – 8697, <https://doi.org/http://dx.doi.org/10.1016/j.jcp.2011.08.008>,
697 <http://www.sciencedirect.com/science/article/pii/S0021999111004803>.
- 698 [45] J. LI AND D. XIU, *Evaluation of failure probability via surrogate models*, Journal of Computational Physics, 229 (2010),
699 pp. 8966 – 8980, <https://doi.org/http://dx.doi.org/10.1016/j.jcp.2010.08.022>, <http://www.sciencedirect.com/science/article/pii/S0021999110004699>.
- 700 [46] M. LI AND Z. WANG, *Deep learning for high-dimensional reliability analysis*, Mechanical Systems and Signal Processing,
701 139 (2020), p. 106399, <https://doi.org/https://doi.org/10.1016/j.ymsp.2019.106399>, <http://www.sciencedirect.com/science/article/pii/S088832701930620X>.
- 702 [47] R. LI AND R. GHANEM, *Adaptive polynomial chaos expansions applied to statistics of extremes in nonlinear random
703 vibration*, Probabilistic Engineering Mechanics, 13 (1998), pp. 125 – 136, [https://doi.org/https://doi.org/10.1016/S0266-8920\(97\)00020-9](https://doi.org/https://doi.org/10.1016/S0266-8920(97)00020-9).
- 704 [48] P.-L. LIU AND A. DER KIUREGHIAN, *Multivariate distribution models with prescribed marginals and covariances*, Probabilistic
705 Engineering Mechanics, 1 (1986), pp. 105–112, [https://doi.org/https://doi.org/10.1016/0266-8920\(86\)90033-0](https://doi.org/https://doi.org/10.1016/0266-8920(86)90033-0),
706 <https://www.sciencedirect.com/science/article/pii/0266892086900330>.
- 707 [49] P.-L. LIU AND K.-G. LIU, *Selection of random field mesh in finite element reliability analysis*, Journal of Engineering
708 Mechanics, 119 (1993), pp. 667–680.
- 709 [50] N. LÜTHEN, S. MARELLI, AND B. SUDRET, *A benchmark of basis-adaptive sparse polynomial chaos expansions for engi-
710 neering regression problems*, 2021, <https://arxiv.org/abs/2009.04800>.
- 711 [51] N. LÜTHEN, S. MARELLI, AND B. SUDRET, *Sparse polynomial chaos expansions: Literature survey and benchmark*, 2021,
712 <https://arxiv.org/abs/2002.01290>.
- 713 [52] S. MARELLI AND B. SUDRET, *An active-learning algorithm that combines sparse polynomial chaos expansions and bootstrap*

- for structural reliability analysis, *Structural Safety*, 75 (2018), pp. 67 – 74.
- [53] J. OAKLEY, *Estimating percentiles of uncertain computer code outputs*, *Journal of the Royal Statistical Society: Series C (Applied Statistics)*, 53 (2004), pp. 83–93, <https://doi.org/10.1046/j.0035-9254.2003.05044.x>, <https://rss.onlinelibrary.wiley.com/doi/abs/10.1046/j.0035-9254.2003.05044.x>, <https://arxiv.org/abs/https://rss.onlinelibrary.wiley.com/doi/pdf/10.1046/j.0035-9254.2003.05044.x>.
- [54] A. B. OWEN, *Monte Carlo theory, methods and examples*, 2013.
- [55] Q. PAN AND D. DIAS, *Sliced inverse regression-based sparse polynomial chaos expansions for reliability analysis in high dimensions*, *Reliability Engineering & System Safety*, 167 (2017), pp. 484 – 493, <https://doi.org/https://doi.org/10.1016/j.ress.2017.06.026>, <http://www.sciencedirect.com/science/article/pii/S095183201630864X>. Special Section: Applications of Probabilistic Graphical Models in Dependability, Diagnosis and Prognosis.
- [56] V. PAPADOPOULOS, D. G. GIOVANIS, N. D. LAGAROS, AND M. PAPADRAKAKIS, *Accelerated subset simulation with neural networks for reliability analysis*, *Computer Methods in Applied Mechanics and Engineering*, 223 (2012), pp. 70 – 80, <https://doi.org/http://dx.doi.org/10.1016/j.cma.2012.02.013>, <http://www.sciencedirect.com/science/article/pii/S0045782512000552>.
- [57] M. PAPADRAKAKIS, V. PAPADOPOULOS, AND N. D. LAGAROS, *Structural reliability analysis of elastic-plastic structures using neural networks and Monte Carlo simulation*, *Computer Methods in Applied Mechanics and Engineering*, 136 (1996), pp. 145–163.
- [58] I. PAPAIOANNOU, M. EHRE, AND D. STRAUB, *Efficient PCE representations for reliability analysis in high dimensions*, in Proceedings of the 19th working conference of the IFIP Working Group 7.5 on Reliability and Optimization of Structural Systems, J. Song, ed., ETH Zürich, 2018.
- [59] I. PAPAIOANNOU, M. EHRE, AND D. STRAUB, *PLS-based adaptation for efficient PCE representation in high dimensions*, *Journal of Computational Physics*, 387 (2019), pp. 186 – 204.
- [60] I. PAPAIOANNOU, S. GEYER, AND D. STRAUB, *Improved cross entropy-based importance sampling with a flexible mixture model*, *Reliability Engineering & System Safety*, 191 (2019), p. 106564.
- [61] I. PAPAIOANNOU, C. PAPADIMITRIOU, AND D. STRAUB, *Sequential importance sampling for structural reliability analysis*, *Structural Safety*, 62 (2016), pp. 66 – 75, <https://doi.org/http://dx.doi.org/10.1016/j.strusafe.2016.06.002>, <http://www.sciencedirect.com/science/article/pii/S0167473016300169>.
- [62] Y. C. PATI, R. REZAIIFAR, Y. C. P. R. REZAIIFAR, AND P. S. KRISHNAPRASAD, *Orthogonal matching pursuit: Recursive function approximation with applications to wavelet decomposition*, in Proceedings of the 27th Annual Asilomar Conference on Signals, Systems, and Computers (1993), 1993, pp. 40–44.
- [63] B. PEHERSTORFER, B. KRAMER, AND K. WILLCOX, *Multifidelity preconditioning of the cross-entropy method for rare event simulation and failure probability estimation*, *SIAM/ASA Journal on Uncertainty Quantification*, 6 (2018), pp. 737–761.
- [64] G. PERRIN, *Adaptive calibration of a computer code with time-series output*, *Reliability Engineering & System Safety*, 196 (2020), p. 106728, <https://doi.org/https://doi.org/10.1016/j.ress.2019.106728>, <https://www.sciencedirect.com/science/article/pii/S0951832018311232>.
- [65] V. PICHENY, D. GINSBOURGER, O. ROUSTANT, R. T. HAFTKA, AND N.-H. KIM, *Adaptive Designs of Experiments for Accurate Approximation of a Target Region*, *Journal of Mechanical Design*, 132 (2010), <https://doi.org/10.1115/1.4001873>, <https://doi.org/10.1115/1.4001873>, <https://arxiv.org/abs/https://asmedigitalcollection.asme.org/mechanicaldesign/article-pdf/132/7/071008/5807381/071008.1.pdf>.
- [66] R. RACKWITZ AND B. FIESSLER, *Structural reliability under combined random load sequences*, *Computers & Structures*, 9 (1978), pp. 489 – 494, [https://doi.org/http://dx.doi.org/10.1016/0045-7949\(78\)90046-9](https://doi.org/http://dx.doi.org/10.1016/0045-7949(78)90046-9), <http://www.sciencedirect.com/science/article/pii/0045794978900469>.
- [67] R. ROSIPAL, *Nonlinear partial least squares: An overview*, *Chemoinformatics and Advanced Machine Learning Perspectives: Complex Computational Methods and Collaborative Techniques*, (2010), <https://doi.org/10.4018/978-1-61520-911-8.ch009>.
- [68] R. Y. RUBINSTEIN AND D. P. KROESE, *Simulation and the Monte Carlo Method*, Wiley Publishing, 3rd ed., 2017.
- [69] K. SARGSYAN, C. SAFTA, H. NAJM, B. J. DEBUSSCHERE, D. RICCIUTO, AND P. THORNTON, *Dimensionality reduction for complex models via Bayesian compressive sensing*, *International Journal for Uncertainty Quantification*, 4 (2014), pp. 63–93.
- [70] R. SCHÖBI, B. SUDRET, AND S. MARELLI, *Rare event estimation using polynomial-chaos Kriging*, *ASCE-ASME Journal of Risk and Uncertainty in Engineering Systems, Part A: Civil Engineering*, 3 (2017), p. D4016002, <https://doi.org/10.1061/AJRUA6.0000870>.
- [71] L. SCHUEREMANS AND D. V. GEMERT, *Benefit of splines and neural networks in simulation based structural reliability analysis*, *Structural Safety*, 27 (2005), pp. 246 – 261, <https://doi.org/http://dx.doi.org/10.1016/j.strusafe.2004.11.001>, <http://www.sciencedirect.com/science/article/pii/S0167473004000529>.
- [72] B. SETTLES, *Active learning literature survey*, Computer Sciences Technical Report 1648, University of Wisconsin–Madison, 2009.
- [73] B. SUDRET, G. BLATMAN, AND M. BERVEILLER, *Response surfaces based on polynomial chaos expansions*, *Construction reliability: Safety, Variability and Sustainability*, (2013), pp. 147–167.
- [74] R. TIPREDDY AND R. GHANEM, *Basis adaptation in homogeneous chaos spaces*, *Journal of Computational Physics*, 259 (2014), pp. 304 – 317, <https://doi.org/https://doi.org/10.1016/j.jcp.2013.12.009>.
- [75] M. E. TIPPING, *Sparse Bayesian learning and the relevance vector machine*, *J. Mach. Learn. Res.*, 1 (2001), p. 211–244.
- [76] J. A. TROPP AND A. C. GILBERT, *Signal recovery from random measurements via orthogonal matching pursuit*, *IEEE Trans. Inf. Theor.*, 53 (2007), p. 4655–4666.
- [77] P. TSLIFIS, X. HUAN, C. SAFTA, K. SARGSYAN, G. LACAZE, J. C. OEFELIN, H. N. NAJM, AND R. G. GHANEM, *Compressive sensing adaptation for polynomial chaos expansions*, *Journal of Computational Physics*, 380 (2019), pp. 29 – 47.
- [78] P. TSLIFIS, I. PAPAIOANNOU, D. STRAUB, AND F. NOBILE, *Sparse polynomial chaos expansions using variational relevance*

- 787 *vector machines*, Journal of Computational Physics, 416 (2020), p. 109498, [https://doi.org/https://doi.org/10.1016/](https://doi.org/https://doi.org/10.1016/j.jcp.2020.109498)
788 <http://www.sciencedirect.com/science/article/pii/S0021999120302722>.
- 789 [79] E. ULLMANN AND I. PAPAIOANNOU, *Multilevel estimation of rare events*, SIAM/ASA Journal on Uncertainty Quantification,
790 3 (2015), pp. 922–953, <https://doi.org/10.1137/140992953>, <https://doi.org/10.1137/140992953>, [https://arxiv.org/abs/](https://arxiv.org/abs/https://doi.org/10.1137/140992953)
791 <https://doi.org/10.1137/140992953>.
- 792 [80] F. URIBE, I. PAPAIOANNOU, Y. M. MARZOUK, AND D. STRAUB, *Cross-entropy-based importance sampling with failure-*
793 *informed dimension reduction for rare event simulation*, SIAM/ASA Journal on Uncertainty Quantification, 9 (2021),
794 pp. 818–847, <https://doi.org/10.1137/20M1344585>.
- 795 [81] P. WAARTS, *Structural Reliability Using Finite Element Analysis: An Appraisal of DARS: Directional Adaptive Response*
796 *Surface Sampling*, PhD thesis, 2000.
- 797 [82] F. WAGNER, J. LATZ, I. PAPAIOANNOU, AND E. ULLMANN, *Multilevel sequential importance sampling for rare event esti-*
798 *mation*, SIAM Journal on Scientific Computing, 42 (2020), pp. A2062–A2087, <https://doi.org/10.1137/19M1289601>.
- 799 [83] Z. WANG AND J. SONG, *Cross-entropy-based adaptive importance sampling using von Mises-Fisher mixture for high di-*
800 *mensional reliability analysis*, Structural Safety, 59 (2016), pp. 42–52.
- 801 [84] S. WOLD, N. KETTANEH-WOLD, AND B. SKAGERBERG, *Nonlinear PLS modeling*, Chemometrics and Intelligent Laboratory
802 Systems, 7 (1989), pp. 53 – 65. Proceedings of the First Scandinavian Symposium on Chemometrics.
- 803 [85] S. WOLD, A. RUHE, H. WOLD, AND W. DUNN III, *The collinearity problem in linear regression. The partial least squares*
804 *(PLS) approach to generalized inverses*, SIAM Journal on Scientific and Statistical Computing, 5 (1984), pp. 735–743.
- 805 [86] C.-F. WU, *Asymptotic Theory of Nonlinear Least Squares Estimation*, The Annals of Statistics, 9 (1981), pp. 501 – 513,
806 <https://doi.org/10.1214/aos/1176345455>.
- 807 [87] D. XIU AND G. E. KARNIADAKIS, *The Wiener–Askey polynomial chaos for stochastic differential equations*, SIAM Journal
808 on Scientific Computing, 24 (2002), pp. 619–644.
- 809 [88] L. YAN, L. GUO, AND D. XIU, *Stochastic collocation algorithms using l_1 -minimization*, International Journal for Uncer-
810 tainty Quantification, 2 (2012), pp. 279–293.
- 811 [89] T. ZHOU AND Y. PENG, *Structural reliability analysis via dimension reduction, adaptive sampling, and Monte Carlo sim-*
812 *ulation*, Structural and Multidisciplinary Optimization, (2020), <https://doi.org/10.1007/s00158-020-02633-0>, <https://doi.org/10.1007/s00158-020-02633-0>.
- 813